A learning experience elicits sex-dependent neurogenomic responses in *Bicyclus anynana* butterflies

Short title: Sexually dimorphic butterfly neurogenomics

David A. Ernst*[1,2], Gabrielle A. Agcaoili*[1], Abbigail N. Merrill[1], Erica L. Westerman[1]

[1]Department of Biological Sciences, University of Arkansas, Fayetteville, AR 72701

[2]Bigelow Laboratory for Ocean Sciences, East Boothbay, ME 04544

*These authors contributed equally

Corresponding Author: Erica L. Westerman; ewesterm@uark.edu; 479-575-5348

Abstract

Sexually dimorphic behavior is pervasive across animals, with males and females exhibiting different mate selection, parental care, foraging, dispersal, and territorial strategies. However, the genetic underpinnings of sexually dimorphic behaviors are poorly understood. Here we investigate gene networks and expression patterns associated with sexually dimorphic imprinting-like learning in the butterfly *Bicyclus anynana*. In this species, both males and females learn visual preferences, but learn preferences for different traits and use different signals as salient, unconditioned cues. To identify genes and gene networks associated with this behavior, we examined gene expression profiles of the brains and eyes of male and female butterflies immediately post training and compared them to the same tissues of naïve individuals. We found more differentially expressed genes and a greater number of associated gene networks in the eyes, indicating a role of the peripheral nervous system in visual imprinting-like learning. Females had higher chemoreceptor expression levels than males, supporting the hypothesized sexual dimorphic use of chemical cues during the learning process. In addition, genes that influence *B. anynana* wing patterns (sexual ornaments), such as *invected*, *spalt*, and *apterous*, were also differentially expressed in the brain and eye, suggesting that these genes may influence both sexual ornaments and the preferences for these ornaments. Our results indicate dynamic and sex-specific responses to social scenario in both the peripheral and central nervous systems and highlight the potential role of wing patterning genes in mate preference and learning across the Lepidoptera.

Key words: mate choice; sexual imprinting; butterfly; transcriptomics; wing patterning

Introduction

Sexually dimorphic behavior is pervasive across animal taxa. Males and females may exhibit different mate selection strategies (Byrne and Rice, 2006; Kokko and Johnstone, 2002; Talyn and Dowse, 2004), parental care behavior (Trivers, 1972; Zilkha et al., 2017), foraging strategies (Ehl et al., 2018; Quillfeldt et al., 2011; Shannon et al., 2006), dispersal (reviewed in (Greenwood, 1980; Trochet et al., 2016)), and territorial displays (Reedy et al., 2017; Rosell and Thomsen, 2006). Though pervasive across species and context, the genetic underpinnings of many types of sexually dimorphic behavior are poorly understood. This is partially because males and females carry much of the same genetic material; thus, sex-specific behavior is unlikely to be allele dependent, except for the rare behaviors that are primarily associated with genes of large effect on the sex chromosome. And, because behaviors are notoriously complex traits, even sexually dimorphic behaviors influenced by genes of large effect on the sex chromosome are likely to also be influenced by autosomal genes of minor effect (Edwards et al., 2009; Lande, 1980).

Substantial headway has been made in elucidating the hormones and genes that act as master regulators of sexually dimorphic traits and behaviors in model systems. Sex-specific steroid hormone production is associated with sexually dimorphic behaviors such as song production in song birds (Alward et al., 2013; Gurney and Konishi, 1980), aggression in mammals (reviewed in (Hashikawa et al., 2018)), and spawning in fish (Pradhan and Olsson, 2015). Similarly, sex-specific alternative splicing of master regulator genes, such as *doublesex*, is associated with sexually dimorphic morphology

and behavior in arthropods (Kunte et al., 2014; Rideout et al., 2007; Rodriguez-Caro et al., 2021; Wang et al., 2022). However, hormones and genes such as *doublesex* are often upstream master regulators, and the presumably sexually dimorphic downstream gene networks associated with hormone- and *doublesex*-related behaviors remain largely unknown, outside of courtship initiation in the fruit fly *Drosophila melanogaster* (Datta et al., 2008; Ruta et al., 2010) and song production in the zebra finch *Taeniopygia guttata* (Olson et al., 2015; Woodgate et al., 2014) and the canary *Serinus canaria* (Alward et al., 2018).

One sexually dimorphic behavior that is pervasive across animals is imprinting-like mate preference learning. In imprinting-like mate preference learning, sexually immature, or juvenile, individuals learn preferences for characteristics of adults (often, but not always parents) of the opposite sex (Immelmann, 1975; ten Cate and Vos, 1999; Verzijden et al., 2012). This behavior is inherently sexually dimorphic, as females learn preferences for male traits, and males learn preferences for female traits (Kendrick et al., 2001; ten Cate, 1985; Verzijden et al., 2008; Witte and Sawka, 2003). The sexual dimorphism in trait learning can be quite extreme if adults are highly sexually dimorphic or there are sex-specific signal modalities, such as male-limited pheromones or song.

To better understand the gene networks underlying sexual dimorphism in imprinting-like learning, we examined sex-specific gene expression patterns in the brains and eyes of *Bicyclus anynana* butterflies during an imprinting-like learning event. Both male and female *B. anynana* butterflies exhibit imprinting-like learning, but they learn preferences for different traits. Female *B. anynana* learn preferences for numbers of dorsal forewing eyespots and are better at learning preferences for increasing numbers of

spots (Westerman et al., 2012). Conversely, male *B. anynana* learn preferences for dorsal hindwing eyespots and are better at learning preferences for loss of spots (Westerman et al., 2014). In addition to the observed sexual dimorphism in traits learned and directionality of learning bias, females learn from males who exude a volatile sex pheromone (Nieberding et al., 2008; Nieberding et al., 2012; Westerman and Monteiro, 2013), while males learn from females who, to our knowledge, do not have a volatile sex pheromone. Thus, the two sexes are likely using different cues as unconditioned stimuli to induce imprinting-like learning.

This sexual dimorphism in learning could be associated with sexual dimorphism in perception, sexual dimorphism in downstream neural processing, or a combination of these two processes. Previous studies suggest that male *B. anynana* have larger eyes and more facets (ommatidia) than female *B. anynana*, and consequently, they potentially have greater spatial acuity (Everett et al., 2012; Macias-Muñoz et al., 2015). If the observed sexual dimorphism in learning is primarily associated with sexual dimorphism in visual perception, we expect to see differential gene expression in the eyes of female and male butterflies and in visual processing genes in the brain. Alternatively, the observed sexual dimorphism in learning could be associated with sex-specific downstream processing, as is seen in *D. melanogaster*'s response to pheromones (Datta et al., 2008; Ruta et al., 2010). In this case we expect to find differential expression of genes unrelated to visual processing in the brains of males and females. We might also find differential expression of putative "magic genes," genes subject to divergent selection that also pleiotropically affect reproductive isolation, potentially by being associated with both the production of and preference for given a trait (Servedio et al., 2011), such as butterfly wing patterning

genes. Many wing patterning genes are expressed in the heads of *B. anynana* (Ernst and Westerman, 2021), and males and females have different wing patterns, with males having brighter UV-reflective eyespots than females (Everett et al., 2012; Prudic et al., 2011) while females have more dorsal hindwing spots than males (Westerman et al., 2014). Additionally, because males but not females produce pheromones that can act as the unconditioned stimuli for learning (Nieberding et al., 2008; Westerman and Monteiro, 2013), we may identify female-specific expression of genes in chemosensory processing pathways.

Materials and Methods

Study Species and Husbandry

Bicyclus anynana is a sub-tropical African butterfly that has been reared in the lab since 1988. The colony at the University of Arkansas was established in spring 2017 from ~1,000 eggs derived from a population in Singapore. Butterflies at the University of Arkansas were reared in a climate-controlled greenhouse at ~27°C, 70% humidity, and under a 13:11h light:dark cycle to mimic wet season conditions and ensure development of the wet season phenotype (Brakefield and Reistma, 1991). Butterflies bred in the laboratory have levels of genetic diversity comparable to those in natural populations, as suggested by similar single-nucleotide polymorphism frequencies found in laboratory and natural populations (Beldade et al., 2006; de Jong et al., 2013).

All adult butterflies used in this study hatched from eggs laid on young corn plants (*Zea mays*) in breeding colony cages containing ~200-500 male and female *B. anynana* butterflies. Plants with eggs were moved to cages containing additional corn

plants for larval consumption, and larvae were fed *ad libitum* until pupation. Upon pupation, pupae were placed in mesh cages (31.8 cm × 31.8 cm × 31.8 cm; Bioquip, Compton, CA, USA) until emergence. Upon emergence, butterflies were transferred to sex- and age-specific cages to isolate the sexes from one another. All butterflies were provided with fresh banana every other day.

Behavioral assays and sample collection

To examine sex-specific gene expression in the brains and eyes of *B. anynana* butterflies during an imprinting-like learning event, both male and female *B. anynana* butterflies were either subjected to an imprinting-like learning event with a conspecific of the opposite sex bearing modified wing ornaments or were placed in a cage alone as a control (Fig. 1A). These two treatments mirror the experiences of trained and naïve individuals prior to mate choice assays in published butterfly imprinting-like learning studies (Westerman et al., 2012; Westerman and Monteiro, 2013; Westerman et al., 2014).

All behavioral assays and sample collection took place between November 2018 - July 2019. Within one hour of dawn, assays were conducted by placing butterflies in a novel mesh cage (39.9 cm × 39.9 cm × 59.9 cm; Bioquip, Compton, CA, USA) for a three-hour observation period (Fig. 1A). Training behavioral assays consisted of either: (1) a newly emerged male paired with a two-day-old, zero-spot female, for which black paint (Enamel Glossy Black 1147, Testors, Rockford, IL, USA) was applied directly on top of her two dorsal hindwing eyespot pupils to block all UV reflectance (for details see (Westerman et al., 2014)) or (2) a newly emerged female paired with a two-day-old, four-

spot male, for which UV-reflective paint (White, FishVision, Fargo, ND, USA) was applied between the two natural dorsal forewing eyespot pupils to create two extra eyespot pupils (for details see (Westerman et al., 2012)). The UV-reflective paint closely replicated the reflectance spectra of natural *B. anynana* eyespot pupils (Westerman et al., 2012). All eyespot manipulations were performed one day prior to behavioral watches. Control assays consisted of either one newly emerged male or one newly emerged female placed in a novel mesh cage (39.9 cm × 39.9 cm × 59.9 cm; Bioquip, Compton, CA, USA) in isolation, as this mirrored the control (naïve) treatment used in prior behavioral assays assessing imprinting-like learning in *B. anynana* butterflies (Westerman et al., 2012; Westerman and Monteiro 2013; Westerman et al., 2014). It is unknown what effect, if any, being paired with a same-sex individual during this time period would have on subsequent mating decisions, thus we did not collect heads from focal animals paired with same-sex individuals. For any given training assay, a control assay using the same sex as the training assay focal animal was conducted concurrently (e.g., for a newly emerged male + zero-spot female training assay, a control assay consisting of a newly emerged male in isolation was run in tandem). All behaviors exhibited by the observed butterflies were recorded using SpectatorGo! (BIOBSERVE; Bonn, Germany). Observed behaviors included: *flutter, fly, walk, rest* (wings closed)*, bask* (wings open greater than 45°)*, antenna wiggle, court* (as defined in (Nieberding et al., 2008))*,* and *copulate*. Because *B. anynana* butterflies have sexually dimorphic wing patterns, these treatments were not conducted blind. However, the behavioral analyses, final RNA-seq analyses, and original observations/head collections were conducted by different people to help reduce potential for observer bias.

After the three-hour behavioral watch, each butterfly's head was removed with RNase-free scissors, transferred into a RNase-free microcentrifuge tube (Biotix; San Diego, CA, USA), and immediately flash frozen in liquid nitrogen. Frozen samples were then stored in a -80^{0}C freezer until dissection and RNA extraction. We collected the heads of ten individuals per group (trained male, trained female, naïve male, and naïve female) to account for variation in response to training, as previous studies suggest that ~75% of females and ~80% of males learn to prefer the trainer phenotype after a three-hour training exposure (Westerman et al., 2012; Westerman et al., 2014).

RNA extraction and cDNA library preparation

To prevent RNA degradation during processing, heads were immersed in 500 µL of pre-chilled RNAlater-ICE (Ambion; Austin, TX, USA) and incubated at -20°C for approximately 18 hours prior to dissection. Thawed heads were then dissected under a dissecting microscope (Zeiss Stemi 508; Jena, Germany) while submerged in RNAlater-ICE to isolate eye and brain tissue. The eyes and brain for each sample were mechanically disrupted separately in lysis buffer using RNase-free, disposable pestles, and small (<200 nucleotides) and large (>200 nucleotides) RNA were extracted separately for each tissue with the NucleoSpin® miRNA kit (Macherey-Nagel; Düren, Germany). RNA quality and quantity were determined using a NanoDrop 2000 (Thermo Fisher Scientific; Waltham, MA, USA), Qubit 2.0 (Invitrogen; Waltham, Massachusetts, USA), and TapeStation 2200 (Agilent; Santa Clara, CA, USA).

Libraries were prepared for the eyes (left and right eye together; n=40) and brain (n=40) for each individual using the KAPA mRNA HyperPrep Kit and Unique Dual-

Indexed Adapters (KAPA Biosystems; Wilmington, MA, USA), with 100 ng of large RNA as input. After running all cDNA libraries on a TapeStation 2200 (Agilent; Santa Clara, CA, USA) and confirming that they were of high quality, libraries were shipped to the University of Chicago Genomics Facility on dry ice. All libraries were subjected to an additional quality assessment using a 5300 Fragment Analyzer (Agilent; Santa Clara, CA, USA), followed by 50 base pair (bp) single end (SE) sequencing across eight lanes of a HiSeq 4000 (Illumina; San Diego, CA, USA).

Read trimming, alignment, and quantification

We concatenated the raw fastq files from all eight lanes for each library and performed an initial quality assessment using FastQC v0.11.5 (http://www.bioinformatics.babraham.ac.uk/projects/fastqc/). One sample (TME_A3, a trained eye sample) failed to sequence properly, so was discarded from downstream analysis. Trimmomatic v0.38 was used to remove any Illumina sequencing adapters from the raw reads (Bolger et al., 2014). We then aligned the adapter-trimmed reads for each sample to the most recent *B. anynana* reference genome (v1.2; (Nowell et al., 2017)) using STAR v2.7.1a (Dobin et al., 2013) and quantified all reads using the "--quantMode GeneCounts" option, which is equivalent to counts produced by the htseq-count script from HTSeq (Anders et al., 2015).

Differential gene expression analyses

The read counts generated by STAR were used as input for the DESeq2 v1.24.0 package (Love et al., 2014) for R (Version 3.6.2, R Foundation for Statistical Computing,

Vienna, Austria) to conduct differential expression analyses. Specifically, we used the generalized linear model design:

$$y \sim sex + condition + sex{:}condition$$

where expression (y) is a function of *sex* (male or female), *condition* (trained or naïve), and their interaction (*sex:condition*). With this design, we made five different tissue-specific comparisons: (1) naïve females vs. naïve males; (2) trained females vs. trained males; (3) trained females vs. naïve females; (4) trained males vs. naïve males; and (5) the interaction of sex and condition. To investigate the overall effect of training while controlling for differences in expression specific to sex, we performed an additional tissue-specific analysis that utilized the design:

$$y \sim sex + condition$$

Only genes with ≥10 total mapped reads were used for the differential expression analyses. Gene expression comparisons were conveyed as the binary log of the expression fold change ($\log_2$FC), with $\log_2$FC shrinkage performed using the ashr method (Stephens, 2017) to obtain more accurate estimates of effect size. Genes were considered differentially expressed if they had a false discovery rate (FDR; (Benjamini and Hochberg, 1995)) < 0.05.

In addition to these standard differential expression analyses, we also performed permutation tests similar to those utilized in Ghalambor et al. (2015) and Bloch et al. (2018). Because this method does not assume gene independence (an unlikely assumption given the nature and abundance of gene co-expression networks), the risk of over-correction is reduced compared to other multiple testing correction methods, resulting in a more accurate representation of the expression data structure (Slonim, 2002). For each

tissue, we randomly assigned both the sex and treatment for each sample to create 1,000 permuted sample phenotype tables. For each of the reassigned sample sets, we ran the DESeq2 analysis exactly as we had for the original analysis, ultimately resulting in a null distribution of 1,000 p-values for every gene. For any given gene, if the p-value from the original analysis was less than the 1% tail of the permuted null distribution, it was considered differentially expressed. Annotations for all differentially expressed genes, including the identified putative vision- and chemsensory-related gene annotations, were extracted from the *B. anynana* reference genome functional annotation from (Ernst and Westerman, 2021).

Weighted gene co-expression network analyses

We performed separate weighted gene co-expression network analyses (WGCNA) for the brain and eyes using the WGCNA v1.70-3 R package (Langfelder and Horvath, 2008) following the WGCNA package developers' recommendations. We first preprocessed the expression data by removing all genes with <10 reads in >90% of the samples to minimize noise from lowly-expressed genes, and a variance-stabilizing transformation was performed on the remaining data using the "varianceStabilizingTransformation" function in DESeq2. Signed co-expression networks for each tissue were constructed by building an adjacency matrix with type = "signed," topological overlap matrix (TOM) with TOMType = "signed," and the soft-thresholding power set to 12 for brains and 14 for eyes. We then identified modules of co-expressed genes using the "cutreeDynamic" function with the following parameters: deepSplit = 2, pamRespectsDendro = FALSE, and minClusterSize = 30. After initial

module identification, we merged modules of high co-expression similarity by first calculating and clustering their eigengenes (the first principal component of a module representing its gene expression profile (Langfelder and Horvath, 2008)) and employing the "mergeCloseModules" function with "cutHeight" set to 0.25.

To identify modules that were significantly associated with any of the sample traits, we used the "binarizeCategoricalVariable" function to create pairwise binary indicators ("traits") for our contrasts of interest (i.e., naïve male vs. naïve female, trained female vs. naïve female, trained male vs. naïve male, and trained female vs. naïve female) and correlated eigengenes with these sample traits. We then adjusted all p-values using the FDR method (Benjamini and Hochberg, 1995), and any module-trait correlations with an FDR <0.05 were considered significant. For all modules that showed significant associations with sample traits, hub genes (genes with the highest connectivity) were identified using the "chooseTopHubInEachModule" function.

For visualization and further analysis, both networks were then exported to Cytoscape v3.8.2 (Shannon et al., 2003) using the "exportNetworkToCytoscape" function with "threshold" set to 0.02. The Cytoscape "Network Analyzer" tool was used to obtain further statistics regarding the connectivity of genes within the networks. Specifically, we calculated three statistics for each gene: (1) degree (the number of other genes connected to a given gene, with a larger number indicating a more highly connected gene), (2) neighborhood connectivity (the average connectivity of all of a gene's neighboring genes), and (3) clustering coefficient (how connected a gene is to its neighboring genes relative to how connected it could be, with "0" representing completely unconnected and "1" representing maximum connectivity).

290

291 *Gene Ontology Analyses*

292 To facilitate the characterization of differentially expressed gene (DEG) sets and
293 significant modules, gene ontology (GO) enrichment analyses were performed using the
294 Fisher's Exact Test function in Blast2GO v5.2.5 (Conesa et al., 2005) with the GO
295 annotations extracted from Ernst and Westerman (2021). In each case, all genes in the
296 expression set (for the WGCNA analysis, all genes that were used in the co-expression
297 analysis) for the respective tissue were used as the reference set, and an FDR threshold of
298 <0.05 was set to identify significantly enriched GO terms. All DEG sets and significant
299 modules were tested for GO enrichment.

300 To further explore the differences between male and female tissues for each
301 condition, we used GOExpress v1.20.0 (Rue-Albrecht et al., 2016) to identify GO terms
302 that best classify the samples from two groups (e.g., female trained brains and male
303 trained brains) based on their gene expression profiles. For these analyses, reads were
304 first normalized to counts per million (CPM) with edgeR v3.28.1 (Robinson et al., 2010),
305 and only genes with ≥1 CPM for at least 10 samples (the maximum number of replicates
306 per group) were retained for the input expression matrix. The random forest was set to
307 10,000 trees, and GO terms that were associated with at least five genes and with a p-
308 value <0.05 after 1,000 permutations were considered significant.

309

310 *Identification of wing patterning genes*

311 In addition to examining differential expression, co-expression networks, and GO
312 signatures, we also investigated the expression patterns of known wing patterning genes,

as these genes have been hypothesized to act as "magic genes" and to have the capacity to influence both preference as well as the preferred trait (Servedio, 2009; Smadja and Butlin, 2011; Westerman, 2019). Specifically, we used the functional annotations and butterfly wing patterning gene list from Ernst and Westerman (2021) to identify wing patterning genes expressed in eye and brain tissue and to determine if they were differentially expressed between the sexes. The genes included numerous *B. anynana* wing patterning genes (Beldade and Peralta, 2017; Bhardwaj et al., 2018; Connahs et al., 2019; Matsuoka and Monteiro, 2018; Monteiro et al., 2013; Monteiro et al., 2006; Monteiro and Prudic, 2010; Ozsu et al., 2017; Prakash and Monteiro, 2018, 2020; Saenko et al., 2011), as well as genes characterized in other butterfly species (Ficarrotta et al., 2022; Martin and Reed, 2010; Nadeau et al., 2016; Reed et al., 2011; Westerman et al., 2018; Woronik et al., 2019).

Analysis of Behavior

We first conducted a Shapiro-Wilk test to assess normality of the behavioral data. We then performed a Kruskal-Wallis test to examine the effect of sex on behavior, followed by a second Kruskal-Wallis test subset by treatment (naïve, trained, and trainer) to test for the effect of sex on behavior in each treatment. We conducted a principal components analysis (PCA) on behavior to search for hidden correlations and create new composite variables (Table S1). We then performed a Kruskal-Wallis test to test for the effect of sex on PC1, PC2, and PC3. We calculated a Bonferroni correction to account for multiple testing, producing an adjusted significance value of $p = 0.0025$.

Ethical Note

All *B. anynana* butterflies were maintained in laboratory conditions as specified by U.S. Department of Agriculture APHIS permit P526P-17-00343. Butterflies not used for this experiment were maintained with ample food and water until natural death.

Results

We sequenced the eye and brain transcriptomes of observed animals, n=10 per treatment per sex, which generated a total of nearly three billion high-quality 50 bp SE reads (Table S2). Approximately 1.6 million reads (0.05% of raw reads) were removed during adapter trimming, with 2.7 billion of the remaining reads (90% of trimmed reads) mapping to the *B. anynana* reference genome (Nowell et al., 2017). Across all brain libraries, 16,785 genes (74% of annotated genes in the genome) had at least 10 mapped reads, while this was the case for 16,612 genes (73%) for eye libraries. For each tissue, these gene sets were used as input for differential expression analyses.

During data quality assessment, gene expression clustering analysis revealed that one sample (TMB_E2, a trained male brain sample) was likely mislabeled, as it clustered with eye samples (Fig. S1). Because the two tissue types exhibited distinct clustering patterns and tissue type accounted for approximately 85% of the variance, this sample was discarded and not included in downstream analyses.

For all differential gene expression comparisons, we used DESeq2 to perform both a standard differential expression analysis as well as a permutation-test-based analysis, a method that eliminates the assumption of gene independence and provides a

more accurate representation of the data structure of gene expression datasets (Bloch et al., 2018; Ghalambor et al., 2015; Slonim, 2002). Nearly all genes that were determined to be differentially expressed in the standard DESeq2 analyses (Tables S3-S14) were also identified as differentially expressed when employing the permutation test analyses (Tables S3-S14). Moreover, because the permutation test analyses reduce potential over-correction by multiple testing correction methods, a larger number of DEGs was found for all comparisons. Therefore, all downstream analyses were conducted with the results of the permutation-based differential expression tests. While all DEG sets obtained from these analyses were tested for GO term enrichment, GO term enrichment results are only reported for DEG sets with significantly enriched GO terms. Behavioral data analyses found similar activity levels across sexes, confirming that sex-specific expression patterns were not the result of sexually dimorphic activity levels (Tables S15 & S16).

Trained male and female brains have distinct expression patterns

Contrasting naïve female and male brains revealed a baseline of 253 genes that were differentially expressed (Fig. 1B,C; Table S3). Conversely, 158 genes were found to be differentially expressed between trained female and male brains (Fig. 1B,C,E; Table S4). Of these gene sets, 127 genes were unique to the training contrast (Fig. 1C), several of which are linked to various neural processes, including neurodevelopment, neural signaling, eye development, and phototransduction (Fig. 2; Table S17). Additionally, four genes with putative chemosensory functions were differentially expressed, all of which were upregulated in females relative to males (chemosensory protein 6, *BANY.1.2.g12995*; ejaculatory bulb-specific protein 3-like, *BANY.1.2.g12992*; ejaculatory

bulb-specific protein 3-like, *BANY.1.2.g12993*; and odorant receptor Or2-like, *BANY.1.2.g25738*) (Ernst and Westerman, 2021). Finally, a gene encoding vitellogenin-like (*BANY.1.2.g11921*), a protein known to influence the social behavior of numerous insect species (Morandin et al., 2019; Nelson et al., 2007; Roy-Zokan et al., 2015), was also upregulated in females.

GOExpress analyses, which find GO terms that best classify samples from two separate groups, identified 171 GO terms that were significantly associated with differences between naïve female and male brains ($p < 0.05$; Table S18), while 166 GO terms differentiated trained female and male brains ($p < 0.05$; Table S19). To eliminate baseline differences, we removed significant terms that were also found in the naïve results, resulting in 51 GO terms linked to differences specific to training (Table S19). Of these terms, several are linked to neural processing, including calmodulin binding ($p = 0.004$), vesicle docking involved in exocytosis ($p = 0.042$), gap junction ($p = 0.046$), and neuropeptide signaling pathway ($p = 0.008$).

Trained male and female eyes have distinct expression patterns

Differential expression analysis found a baseline of 443 genes that were differentially expressed between naïve female and male eyes (Fig. 1B,D; Table S5). By contrast, 180 DEGs were found for the trained female vs. male comparison (Fig. 1B,D,F; Table S6). In total, 142 genes were unique to the trained eye contrast (Fig. 1D), including genes encoding proteins linked to neurodevelopment, neural signaling, hormone signaling, and vision (Fig. 2; Table S17). Moreover, three genes putatively linked to circadian rhythms showed differential expression, including circadian clock-controlled

protein-like (*BANY.1.2.g04378*), which was upregulated in males, and circadian clock-controlled protein-like (*BANY.1.2.g05915*) and protein takeout-like (*BANY.1.2.g05914*), which were both upregulated in females. The takeout gene (*to*) is also associated with male courtship behavior in *D. melanogaster* (Dauwalder et al., 2002), making its upregulation in sexually immature *B. anynana* females during a training period intriguing.

GOExpress analyses revealed 165 and 138 GO terms that were significantly linked to expression differences between the sexes for naïve and trained eyes, respectively ($p < 0.05$; Tables S20, S21). Removal of terms that overlapped both the naïve and trained sets resulted in 37 GO terms linked to sex-specific differences in response to training (Table S21). A number of these terms were associated with neural processes and sensory transduction, including chloride transmembrane transport ($p = 0.007$), chloride channel activity ($p = 0.01$), vesicle docking involved in exocytosis ($p = 0.017$), and G protein-coupled peptide receptor activity ($p = 0.025$).

Training has sex-dependent effects on expression patterns in brains and eyes

Sex-specific pairwise comparisons between trained and naïve tissues revealed many DEGs in all sex-dependent comparisons.

Starting with the female comparisons, a total of 135 genes were found to be differentially expressed between trained and naïve female brains (Fig. 1B,C; Table S7), many of which have potential roles in neural development, neural signaling, hormone metabolism, and eye-related processes (Fig. 2; Table S17).

For the trained vs. naïve female eyes comparison, differential expression analysis identified 291 DEGs (Fig. 1B,D; Table S8). GO enrichment analysis found 12 GO terms enriched in this gene set, with the top being mitochondrion (FDR=4.04×10^{-4}), intracellular organelle (FDR=4.04×10^{-4}), and organelle (FDR=5.23×10^{-4}) (Table S22). There were several genes of interest in the trained vs. naïve female eye contrast, including genes linked to neural development and signaling, hormone signaling, eye development, and vision (Fig. 2; Table S17).

Similar to the female brains comparison, the trained vs. naïve male brains comparison found 135 DEGs (Fig. 1B,C; Table S9), including several genes associated with neurodevelopment, neural signaling, and eye development (Fig. 2; Table S17).

Differential expression analysis revealed 243 DEGs for the trained vs. naïve male eyes comparison (Fig. 1B,D; Table S10). Again, numerous genes involved with neural development, neural signaling, hormone signaling, vision, and eye development were found to be differentially expressed between trained and naïve male eyes (Fig. 2; Table S17).

Moreover, 63 genes in the brain and 80 genes in the eye were found to have a significant sex:condition interaction, indicating that training differentially affected their expression in females versus males (Fig. 1B,C,D; Tables S11, S12). In both tissues, these sex:condition interactions were found for genes involved with neural development and signaling, and interactions were also found for genes linked to eye development in the eye comparison (Table S17). In addition, a gene putatively involved with chemoreception (olfactory receptor 21, *BANY.1.2.g12009*; (Ernst and Westerman, 2021)) and a gene associated with regulating circadian rhythms (protein LSM12 homolog,

450 *BANY.1.2.g13734*; (Lee et al., 2017)) showed significant sex:condition interactions in the
451 brain and eyes, respectively.
452
453 *Training has a sex-independent effect on gene expression in brains*
454 Testing for the overall effect of training while controlling for differences in
455 expression due to sex revealed 283 genes that were differentially expressed in trained vs.
456 naïve brains (Fig. S2A; Table S13). Many of the genes in this gene set have functions
457 related to neurodevelopment, neural signaling, hormone signaling, and eye development
458 (Fig. 2; Table S17). Moreover, LSM12 homolog (*BANY.1.2.g13734*), which showed a
459 significant sex:condition interaction in the eyes, was also differentially expressed and was
460 upregulated in naïve brains.
461
462 *Training has a sex-independent effect on gene expression in eyes*
463 In total, 658 DEGs were identified for the trained vs. naïve eyes comparison when
464 controlling for sex (Fig. S2B; Table S14). GO enrichment analysis revealed 30 enriched
465 GO terms, with the top terms being mitochondrion (FDR=1.92×10^{-6}), protein-containing
466 complex (FDR=3.03×10^{-6}), and intracellular organelle (FDR=5.17×10^{-6}) (Table S23).
467 Several of these DEGs have putative functions in neurodevelopment, neural
468 signaling, hormone signaling, eye development, and vision (Fig. 2; Table S17). In
469 addition, a number of genes linked to learning and memory were differentially expressed
470 between trained and naïve eyes. Several of these genes were upregulated in trained eyes,
471 including nipped-B protein (*BANY.1.2.g01712*), Ca(2+)/calmodulin-responsive adenylate
472 cyclase (*BANY.1.2.g01825*), transcription factor Adf-1-like (*BANY.1.2.g03430* and

473 *BANY.1.2.g08959*), adenylate cyclase type 8 (*BANY.1.2.g03804*), neurobeachin-like
474 (*BANY.1.2.g12252* and *BANY.1.2.g12258*), and ataxin-2 homolog isoform X1
475 (*BANY.1.2.g13668*). Conversely, cyclic AMP response element-binding protein B
476 isoform X3 (*BANY.1.2.g01685*), transcription factor Adf-1-like (*BANY.1.2.g24076),*
477 probable RNA helicase armi isoform X1 (*BANY.1.2.g17424*), and fatty acid-binding
478 protein-like (*BANY.1.2.g17524*) were upregulated in naïve eyes. Finally, two genes
479 involved with male courtship in *Drosophila* (calcium/calmodulin-dependent 3',5'-cyclic
480 nucleotide phosphodiesterase 1 isoform X1, *BANY.1.2.g07806*; and cytoplasmic dynein 2
481 heavy chain 1, *BANY.1.2.g19627*) were upregulated in *B. anynana* eyes in the training
482 condition.
483
484 *One gene network is associated with training condition in the brain*
485 To investigate gene networks that are associated with an imprinting-like learning
486 experience, we performed tissue-specific WGCNAs. Brain co-expression network
487 analysis identified 17 modules, which was reduced to 11 after merging highly correlated
488 modules (Fig. 3A; Fig. S3A). Of these modules, only one (the red module) was
489 significantly correlated with a trait, specifically the trained male brain vs. naïve male
490 brain contrast (i.e., the red module was significantly correlated with training condition for
491 male brains; r=0.6; FDR=0.004) (Fig. 3C; Fig. S3B). This module consisted of 655 genes
492 (Table S24), with the top hub gene (i.e., the most highly connected gene) identified as
493 NADH dehydrogenase [ubiquinone] 1 beta subcomplex subunit 7-like
494 (*BANY.1.2.g00209*). GO enrichment analyses found five significantly enriched GO terms

in the red module, which were linked to nucleic acid and cyclic compound binding and mRNA metabolism (Table S25; Fig. 4A).

Many genes within the red module are linked to various neural and sensory processes. Of particular interest, 41 DEGs identified in the trained vs. naïve male brain contrast were also present in the red module network (Table S24). Many of these genes encode proteins linked to neural development, such as protein smoothened (*BANY.1.2.g01253*), protein abrupt-like isoform X5 (*BANY.1.2.g17381*), histone acetyltransferase Tip60 isoform X6 (*BANY.1.2.g17798*), Down syndrome cell adhesion molecule-like protein (*BANY.1.2.g23099*), Down syndrome cell adhesion molecule-like protein CG42256 (*BANY.1.2.g23100*), and helicase domino (*BANY.1.2.g24509*). Additionally, others encode proteins involved with neural signaling, such as piezo-type mechanosensitive ion channel component isoform X1 (*BANY.1.2.g11981*) and V-type proton ATPase subunit a (*BANY.1.2.g18298*) and eye development, such as *trr*, (*BANY.1.2.g04855*) and *crb* (*BANY.1.2.g13186*) (Table S17). In addition to its role in eye development, *trr* is also involved with short term courtship memory in *D. melanogaster* (Sedkov et al., 2003).

Several gene networks are associated with training condition in the eyes

Eye co-expression network analysis identified 20 modules, which was reduced to 13 after merging highly correlated modules (Fig. 3B, Fig. S4A). Of these modules, seven (the black, blue, cyan, grey60, magenta, midnight blue, and tan modules) were significantly correlated with at least one contrast, and DEGs for the correlated contrast(s) were present in all seven of these modules (Fig. 3D, Fig. S4; Tables S26-S38).

Two of these modules (the black and magenta modules), both of which were significantly correlated with the trained male vs. naïve male eyes contrast, were of particular interest based on their GO enrichment profiles. The black module (r=0.66; FDR=2.00×10^{-4}) consisted of 366 genes centered around the top hub gene gamma-aminobutyric acid type B receptor subunit 2 (*BANY.1.2.g00039*), a component of the receptor for the neurotransmitter GABA (S27 Table; Fig. 3D, Fig. S4C). Moreover, 73 GO terms were enriched in this module, most of which are associated with neural processes (e.g., neurotransmitter receptor activity involved in regulation of postsynaptic membrane potential, chemical synaptic transmission, and excitatory postsynaptic potential) (Table S29; Fig. 4B). A total of 32 DEGs from the trained male vs. naïve male eyes contrast were found in the black module, nearly half of which are associated with neural and eye development and neural signaling. Differentially expressed development genes include protein unc-80 homolog isoform X10 (*BANY.1.2.g05052*), microtubule-associated protein futsch-like (*BANY.1.2.g08693*), delta and Notch-like epidermal growth factor-related receptor (*BANY.1.2.g09881*), protein abrupt-like isoform X1 (*BANY.1.2.g17383*), and *rst* (*BANY.1.2.g15359*) (Table S17; Table S28). Moreover, differentially expressed neural signaling genes include sodium channel protein para (*BANY.1.2.g00003*), potassium voltage-gated channel subfamily KQT member 1 isoform X2 (*BANY.1.2.g01557*), adenylate cyclase type 8 (*BANY.1.2.g03804*), neuroligin-4, Y-linked isoform X1 (*BANY.1.2.g06479*), acetylcholine receptor subunit alpha-like 2 (*BANY.1.2.g06669*), potassium channel subfamily T member 2 isoform X10 (*BANY.1.2.g09307*), calcium/calmodulin-dependent protein kinase kinase 1 (*BANY.1.2.g12425*), sodium leak channel non-selective protein (*BANY.1.2.g19402*),

gamma-aminobutyric acid type B receptor subunit 2 isoform X3 (*BANY.1.2.g21830*), and dopamine receptor 2-like, (*BANY.1.2.g24500*) (Table S17; Table S28).

The magenta module (r=0.59; FDR=0.002) consisted of 417 genes with a hub gene of disintegrin and metalloproteinase domain-containing protein 33-like (Fig. S4D; Table S30) and showed an enriched GO term profile similar to that of the black module (Fig 4C; Table S31). Specifically, the terms transmembrane signaling receptor activity, G protein-coupled receptor signaling pathway, G protein-coupled receptor activity, signaling receptor activity, and molecular transducer activity were found to be enriched in both the black and magenta modules. In total, 21 DEGs from the trained male vs. naïve male eyes contrast were found in the magenta module, a third of which have putative functions in neurodevelopment (protein smoothened isoform X2, *BANY.1.2.g01254*; putative defective proboscis extension response, *BANY.1.2.g12002*; rho GTPase-activating protein 100F, *BANY.1.2.g12733*; and dynamin-like 120 kDa protein, mitochondrial, *BANY.1.2.g23042*), neural signaling (regulating synaptic membrane exocytosis protein 1 isoform X1, *BANY.1.2.g10739*; and dopamine receptor 1, *BANY.1.2.g24271*), and eye development (adenylyl cyclase-associated protein 1 isoform X1, *BANY.1.2.g04305*) (Tables S17, S30).

Wing patterning genes are differentially expressed in both the brain and eyes

To investigate whether putative "magic genes," or genes that influence both a given trait as well as preference for that trait, are expressed in the brain and eyes of *B. anynana*, we also explored the expression patterns of known butterfly wing patterning genes. A total of 53 wing patterning genes were found to be expressed in the brain, while

50 were expressed in the eyes (Table S39). Although none of these wing patterning genes exhibited sex-specific expression (meaning only expressed in one sex) in either tissue, 46 were in common across the two tissues. Seven genes showed brain-specific expression, including homologs for cortex (*BANY.1.2.g04256*), engrailed (*BANY.1.2.g14935*), CD63-antigen (*BANY.1.2.g12556*), aristaless (*BANY.1.2.g21346* and *BANY.1.2.g24453*), and BarH-1 (*BANY.1.2.g19326* and *BANY.1.2.g22154*), while four exhibited eye-specific expression, including homologs for hedgehog (*BANY.1.2.g04016*) and CD63-antigen (*BANY.1.2.g20540*, *BANY.1.2.g25497*, and *BANY.1.2.g25594*).

Several wing patterning genes were identified as differentially expressed for various contrasts, including between and within sexes, in both tissue types. For the naïve female vs. male brain contrast, sal-like protein 1 (*BANY.1.2.g09547*) and CD63 antigen-like (*BANY.1.2.g23713*) were both upregulated in females (Fig. 5, Table S3). In the trained female vs. male brain contrast protein apterous-like isoform X2 (*BANY.1.2.g08342*) was upregulated in males (Fig. 5, Table S4). In the naïve female vs. male eye contrast CD63 antigen-like (*BANY.1.2.g25497*) was upregulated in females (Fig. 5, Table S5). Moreover, in the eye interaction contrast CD63 antigen-like (*BANY.1.2.g25497*) was upregulated in trained females and naive males (Fig. 5, Table S12), and in the trained vs. naïve eye controlling for sex contrast CD63 antigen-like isoform X2 (*BANY.1.2.g10818*) was upregulated in naïve eyes (Fig. 5, Table S14).

When comparing within sexes, three known wing patterning genes were differentially expressed in male brains or eyes. In the trained vs. naïve male brain contrast, protein bric-a-brac 2-like isoform X4 (*BANY.1.2.g17823*) was upregulated in trained males while Homeobox protein invected (*BANY.1.2.g18817*) was upregulated in

587 naïve males (Fig. 5, Table S9). By contrast, in the trained vs. naïve male eye comparison
588 protein apterous-like isoform X2 (*BANY.1.2.g08342*) was upregulated in trained males
589 (Fig. 5, Table S10). No known wing patterning genes were differentially expressed in
590 female-specific contrasts.
591
592 **Discussion**
593 Here we identified a number of genes that were differentially expressed in the
594 brains and eyes of females and males during an imprinting-like learning event, as well as
595 several associated gene networks. We found DEGs in both tissue types, suggesting that
596 imprinting-like learning, and sexually dimorphic aspects of this learning process, are
597 associated with transcriptional changes in both the peripheral sensory system and the
598 brain. A number of chemosensory genes were upregulated in females relative to males,
599 supporting the hypothesized female-specific use of pheromones in the mate preference
600 learning process (Westerman and Monteiro, 2013; Westerman et al., 2014). Furthermore,
601 a suite of butterfly wing patterning genes, which have long been hypothesized to also
602 influence mate preference and potentially serve as "magic genes," were also differentially
603 expressed in the eyes and brains of *B. anynana* butterflies during training events, further
604 supporting their hypothesized role in mate preference and speciation.
605 One of the more interesting aspects of sexually dimorphic imprinting-like learning
606 in *B. anynana* is the presence/absence of sex pheromones in males versus females.
607 Previous studies have shown that the male sex pheromone is an indicator of age
608 (Nieberding et al., 2012), is species-specific (Bacquet et al., 2015; Nieberding et al.,
609 2008), is equally weighted with visual signals during female mate selection (Costanzo

and Monteiro, 2007), and influences the valence females learn to associate with visual signals during imprinting-like learning (Westerman and Monteiro, 2013). Thus, male chemical cues are known to be important for female mate choice in this system. On the other hand, a sex pheromone has not been discovered in female *B. anynana*, and it remains unclear what unconditioned stimulus males use to assign positive valence to number of hindwing spots. The results of this study appear to support this sex-specific use of olfactory signals during the learning process. The most clear-cut finding supporting this hypothesis is that chemosensory genes, including an odorant receptor, are upregulated in females relative to males during the training period. Odorant receptors are differentially expressed in response to training in other species that rely on olfactory signals during mate preferences, such as female *Xiphophorus malinche* swordtail fish (Cui et al., 2017) and male and female mice (*Mus musculus*) (Broad and Keverne, 2012). While both sexes of *M. musculus* learn olfactory signals and exhibit olfaction-associated differential gene expression after early odor exposure, it is unknown whether male *X. malinche* fish respond to training with olfactory cues, or whether subsequent differential expression of odorant receptors is sexually dimorphic. It would be interesting to see if the sexual dimorphism in chemosensory gene expression we observed in *B. anynana* also occurs in swordtail fish, or whether these patterns are more similar to mice, given that both male and female swordtails exude olfactory signals (Cui et al., 2017; Wong et al., 2005).

A second result that may be related to the differential use of olfactory cues during the learning (and mate choice) process is that we found a larger set of gene networks associated with the training condition in the brains and eyes of males than in females.

633 This could be a result of imprinting-like learning being more consistent in males than
634 females (80% vs 75% prefer the trainer phenotype) (Westerman et al., 2012; Westerman
635 et al., 2014). However, it could also be a side effect of females relying more heavily on
636 olfactory signals than males, as we did not include antennae in our analyses and
637 consequently may have missed learning-associated gene networks that reside in female
638 antennae. Female *Heliconius melpomene* and *Heliconius cydno* butterflies are sensitive to
639 male pheromones (Byers et al., 2020) and exhibit different antennae expression profiles
640 before and after copulation as well as sex-specific expression profiles (van Schooten et
641 al., 2020). It would be interesting to see if *B. anynana* females exhibit training-specific,
642 sexually dimorphic antennae expression profiles that correspond to their sex-specific
643 emphasis on olfactory signals during the preference learning and mate selection process.
644 While the gene expression patterns of the antennae are unknown for these
645 animals, we did find training-specific, sexually dimorphic gene expression patterns in *B.*
646 *anynana* eyes. Because female and male *B. anynana* butterflies learn preferences for
647 different visual signals and exhibit visual learning biases in different directions (gains and
648 losses, respectively (Westerman et al., 2012; Westerman et al., 2014)), one of our
649 hypotheses was that we would see sexually dimorphic expression of vision-related genes
650 during the learning process, especially in the eyes. Although we did not observe
651 differential expression of any opsins, we did find sex-dependent expression patterns of a
652 number of vision-related genes, including an ommochrome-binding protein, retinol
653 dehydrogenase 11, rhodopsin kinase 1 (*Gprk1*), and arrestin homolog isoform X2.
654 Ommochrome pigments act as filtering pigments in the eyes of butterflies, limiting the
655 wavelengths of light a butterfly can see (Arikawa and Stavenga, 2014; Stavenga, 2002).

These filtering pigments are sexually dimorphic in a number of different species, including *H. cydno*, *H. melpomene*, *Heliconius pachinus*, and *Colias erate*, and are hypothesized to influence mate choice in these systems (Buerkle et al., 2022; Ogawa et al., 2013). It remains unclear whether filtering pigment type or distribution is sexually dimorphic in *B. anynana*, or whether filtering pigment production or distribution in the eye is plastic in response to circadian rhythms, social scenario, or age. However, our findings of socially-dependent expression patterns of ommochrome-binding protein and a number of other vision-related genes suggest that vision is highly dynamic, not just in the context of light environment (Obara et al., 2008; Sakai et al., 2018; Wright et al., 2020) and circadian rhythms (Li et al., 2008; Li et al., 2005), but also in response to social environment.

In addition to finding vision-associated differentially expressed genes, a number of learning and memory genes were differentially expressed during training/imprinting, specifically in the eyes, including dopamine receptors. This pattern is strongest in males, though it is also observed when the data for both sexes are pooled. Moreover, the most highly connected gene for a gene network associated with training condition in male eyes (the black module) encodes a component of the receptor for the neurotransmitter GABA, gamma-aminobutyric acid type B receptor subunit 2. This network also contained a variety of genes involved with neural processing that were differentially expressed between trained and naïve male eyes, including additional neurotransmitter receptors (acetylcholine receptor subunit alpha-like 2, gamma-aminobutyric acid type B receptor subunit 2 isoform X3, and dopamine receptor 2-like). While there is some debate over whether eyes should be considered part of the peripheral nervous system or the central

679 nervous system in vertebrates (London et al., 2013), there has been less attention given to
680 the potentially broad cognitive role of the retina in comparison to the optic lobe in insects
681 (as illustrated by (Perry et al., 2017)). Our findings indicate that transcription in the
682 butterfly eye changes in response to social scenario (presence/absence of a sexually
683 mature conspecific of the opposite sex) and that this change includes the transcription of
684 genes associated with higher processing. These results suggest that neurogenomic
685 processes associated with cognition might not be limited to the optic lobe and central
686 brain in insects, but might also occur in the retina. It is interesting to note that dopamine
687 is not only important for learning (Schwaerzel et al., 2003), but is also critical for eye
688 development (reviewed in (Zhou et al., 2017)) and consequently may influence visual
689 learning in *B. anynana* butterflies in both sensory processing and higher processing
690 pathways. The differential expression of dopamine receptors in males but not females
691 further supports the hypothesis that males may be placing greater emphasis on visual
692 signals than females during these social encounters.

693 It is important to keep in mind that we compared the transcriptomes of males and
694 females during social experiences that induce learning with the transcriptomes of naïve
695 individuals of the same age; we did not collect transcriptomic data for males and females
696 during mixed-sex social experiences that do not induce learning or during social
697 experiences with individuals of the same sex. Thus, some of the DEGs that we observed
698 are likely to be associated with sexually dimorphic responses to social interactions, not
699 learning per se, as has been previously shown in female *Xiphophorus* swordtail fish
700 (Cummings et al., 2008). It would be interesting to see if early social experience with
701 sexually mature individuals of the same sex also influences future mate choice, as that

has not been tested in this system (Westerman et al., 2012; Westerman & Monteiro 2013; Westerman et al., 2014). It would also be intriguing to investigate whether exposure to sexually mature individuals with wing patterns that are difficult to learn (e.g., 0 spots for females and 2 spots for males) results in different suites of DEGs in the brain and/or eyes of either sex. Moreover, it would be worthwhile to explore if similar suites of genes are expressed in sexually mature females and males in a sexually dimorphic manner, as the current experiment focused on females and males that were sexually immature (the training period in this study occurs prior to sexual receptivity in both sexes (Westerman et al., 2012; Westerman et al., 2014)).

Broad role of sensory receptors and neurotransmitters in sexually dimorphic behavior

Although neurogenomic assessment of sexually dimorphic behavior is relatively rare to date, similarities between our results and those in other animal systems suggest common mechanisms may underlie sexually dimorphic behavior across animal taxa. Sensory receptors seem to be especially important and connected to downstream sexually dimorphic gene networks. For example, odorant receptor expression influences female receptivity and male ability to differentiate between the sexes in *D. melanogaster* (Datta et al., 2008), male and female zebra finches exhibit different brain gene expression profiles when listening to the same song (Gobes et al., 2009), a number of butterfly species exhibit sexually dimorphic opsin expression patterns (Buerkle et al., 2022; Everett et al., 2012), and *B. anynana* exhibit sexually dimorphic chemical receptor expression during a mate preference learning event (this study). Sexually dimorphic catecholamine-associated expression (receptors or binding proteins, for example) also

appears to be important for driving sexually dimorphic social behaviors across taxa, as illustrated by sex-dependent distribution of tyrosine hydroxylase in male and female plainfin midshipman fish brains (Goebrecht et al., 2014) and sexually dimorphic association of dopamine receptors and binding proteins with social interactions in *B. anynana* butterflies (this study). Pathways integrating sensory receptors and catecholamine neurotransmitters may be particularly fruitful for future study of sexually dimorphic behaviors across animal taxa.

Wing patterning genes may be "magic" genes

While butterfly wing patterning genes have long been hypothesized to play a role in shaping both wing pattern and preference for wing pattern (Kronforst and Papa, 2015; Kronforst et al., 2006; Merrill et al., 2015; Merrill et al., 2019; Naisbit et al., 2001), evidence supporting this hypothesis has been rare. However, wing pattern elements (eyespots, specific colors, and specific patterns) are known sexual ornaments in many butterfly species (Ellers and Boggs, 2003; Ficarrotta et al., 2022; Jiggins et al., 2001; Kronforst et al., 2006; Obara et al., 2008; Robertson and Monteiro, 2005; Westerman et al., 2019), and the genes underlying a number of these sexual ornaments have been functionally characterized (Ficarrotta et al., 2022; Kunte et al., 2014; Matsuoka and Monteiro, 2018; Monteiro et al., 2013; Nadeau et al., 2016; Ozsu et al., 2017; Reed et al., 2011; Westerman et al., 2018) (please note that neither of these citation lists are exhaustive). Thus, butterflies are a great system for testing the hypothesis that genes influencing sexual ornamentation may also influence preference for those sexual ornaments. Here we show that a number of wing patterning genes are differentially

748 expressed in the brain and eyes during a sexual (training) encounter. Not only are these
749 genes associated with wing patterning in a range of butterfly species, but a subset of these
750 genes are specifically associated with aspects of eyespot production in *B. anynana*
751 (Brunetti et al., 2001; Ozsu and Monteiro, 2017; Prakash and Monteiro, 2018) and/or
752 with UV reflectance (Ficarrotta et al., 2022). Because male and female *B. anynana* learn
753 preferences for eyespot number, and specifically the UV-reflective center of the eyespots
754 (Westerman et al., 2012; Westerman et al., 2014), these genes that both influence
755 eyespots or UV scale production and are differentially expressed in the brain or eyes
756 during an intersexual social encounter (*invected*, *spalt*, *apterous*, *CD63 antigen-like*, and
757 *bric-a-brac*) are particularly promising candidate magic genes in the *B. anynana* system.
758 The brain and eye expression profiles of genes known to influence wing patterning traits
759 important for mate selection in other butterfly systems, such as *BarH-1* (Woronik et al.,
760 2019), *artistaless* (Westerman et al., 2018), *cortex* (Nadeau et al., 2016), and *doublesex*
761 (Kunte et al., 2014), support the hypothesis that these genes may be expressed in the
762 brains or eyes of the butterfly species using these genes to control wing pattern elements
763 under sexual selection. Future studies should explore the pervasiveness of genes
764 influencing both wing pattern (sexual ornamentation) and mate preference across the
765 Lepidoptera.
766
767 **Conclusions**
768 Here we show that sexually dimorphic, imprinting-like learning is associated with
769 sexually dimorphic gene expression in the brains and eyes of *B. anynana* butterflies
770 during a training event. Differentially expressed genes include sensory receptors and

genes associated with neurotransmitters in both tissue types, indicating dynamic and sex-specific responses to social scenario in both the peripheral and central nervous systems. Sexually dimorphic expression of chemosensory genes supports the role of pheromones in female but not male imprinting-like learning, while the learning-related expression of numerous wing patterning genes highlight the potential for these genes to influence both wing pattern and mate preference. Future research should explore the gene and neural networks bridging sexually dimorphic sensory receptors to sexually dimorphic behavior, and determine the functional role of wing patterning genes in mate preference in other lepidopterans.

Acknowledgements

We thank Matthew Murphy, Grace Hirzel, Deonna Robertson, and Sushant Potdar for assistance with animal husbandry. This research was supported by NSF IOS grant #1937201 to ELW, an Arkansas Biosciences Institute (the major research component of the Arkansas Tobacco Settlement Proceeds Act of 2000) grant to ELW, a University of Arkansas Honors College grant to GAA & ELW, the Arkansas High Performance Computing Center, which is funded through multiple NSF grants and the Arkansas Economic Development Commission, and the University of Arkansas.

Competing Interests: The authors declare no competing interests.

Literature Cited

Alward BA, Balthazart J, Ball GF, 2013. Differential effects of global versus local testosterone on singing behavior and its underlying neural substrate. Proceedings of the National Academy of Sciences 110:19573-19578. doi: 10.1073/pnas.1311371110.

Alward BA, Cornil CA, Baltharzart J, Ball GF, 2018. The regulation of birdsong by testosterone: Multiple time-scales and multiple sites of action. Hormones and Behavior 104:32-40. doi: 10.1016/j.yhbeh.2018.04.010.

Anders S, Pyl PT, Huber W, 2015. HTSeq— a Python framework to work with high-throughput sequencing data. Bioinformatics 31:166-169. doi: 10.1093/bioinformatics/btu.

Arikawa K, Stavenga DG, 2014. Insect photopigments: Photoreceptor spectral sensitivities and visual adaptations. In: Hunt DMea, editor. Evolution of Visual and Non-visual Pigments New York: Springer Science + Business p. 137-162.

Bacquet PMB, Brattstrom O, Wang H-L, Allen C, Lofstedt C, Brakefield PM, Nieberding CM, 2015. Selection on male sex pheromone composition contributes to butterfly reproductive isolation. Proceedings of the Royal Society of London B 282:20142734. doi: 10.1098/rspb.2014.2734.

Beldade P, Peralta CM, 2017. Developmental and evolutionary mechanisms shaping butterfly eyespots. Current Opinion in Insect Science 19:22-29. doi: 10.1016/j.cois.2016.10.006.

Beldade P, Rudd S, Gruber JD, Long AD, 2006. A wing expressed sequence tag resournce for *Bicyclus anynana* butterflies, an evo-devo model. BMC Genomics 7. doi: 10.1186/1471-2164-7-130.

Benjamini Y, Hochberg Y, 1995. Controlling the false discovery rate: a practical and powerful approach to multiple testing. Journal of the Royal Statistical Society Series B (Methodological) 57:289-300.

Bhardwaj S, Prudic KL, Bear A, Dasgupta M, Wasik BR, Tong X, Cheong WF, Wenk MR, Monteiro A, 2018. Sex Differences in 20-Hydroxyecdysone hormone levels control sexual dimorphism in *Bicyclus anynana* wing patterns. Molecular Biology and Evolution 35:465-472. doi: 10.1093/molbev/msx301.

Bloch NI, Corral-López A, Buechel SD, Kotrschal A, Kolm N, Mank JE, 2018. Early neurogenomic response associated with variation in guppy female mate preference. Nature Ecology and Evolution 2:1772-1781. doi: 10.10378/s41559-018-0682-4.

Bolger AM, Lohse M, Usadel B, 2014. Trimmomatic:a flexible trimmer for Illumina sequence data. Bioinformatics 30:2114-2120. doi: 10.1093/bioinformatics/btu170.

Brakefield PM, Reistma N, 1991. Phenotypic plasticity, seasonal climate and the population biology of *Bicyclus* butterflies (Satyridae) in Malawi. Ecological Entomology 16:291-303.

Broad KD, Keverne EB, 2012. The post-natal chemosensory environment induces epigenetic changes in vomeronasal receptor gene expression and a bias in olfactory preference. Behavior Genetics 42:461-471. doi: 10.1007/s10519-011-9523-9.

Brunetti CR, Selegue JE, Monteiro A, French V, Brakefield PM, Carroll SB, 2001. The generation and diversification of butterfly eyespot color patterns. Current Biology 11:1578-1585. doi: 10.1016/S0960-9822(01)00502-4.

Buerkle N, Westerman EL, Kronforst MR, Palmer SE, 2022. Sex-limited diversification of the eye in *Heliconius* butterflies. bioRxiv. doi: 10.1101/2022.04.25.489414.

Byers KJRP, Barragh K, Musgrove J, Almeida DA, Garza SF, Warren IA, Rastas PM, Kucka M, Chan YF, Merrill RM, Schultz S, McMillan WO, Jiggins CD, 2020. A major locus controls a biologically active pheromone component in *Heliconius melpomene*. Evolution 74:349-364. doi: 10.1111/evo.13922.

Byrne PG, Rice WR, 2006. Evidence for adaptive male mate choice in the fruit fly *Drosophila melanogaster* Proceedings of the Royal Society of London B 273:917-922. doi: 10.1098/rspb.2005.3372.

Conesa A, Götz S, García-Gómez JM, Terol J, Talón M, Robles M, 2005. Blast2GO: a universal tool for annotation, visualization and analysis in functional genomics research. Bioinformatics 21:3674-3676. doi: 10.1093/bioinformatics/bti610.

Connahs H, Tlili S, van Creij J, Loo TYJ, Banerjee TD, Saunders TE, Monteiro A, 2019. Activation of butterfly eyespots by Distal-less is consistent with a reaction-diffusion process. Development 146:146. doi: 10.1242/dev.169367.

Costanzo K, Monteiro A, 2007. The use of chemical and visual cues in female choice in the butterfly *Bicyclus anynana*. Proceedings of the Royal Society of London B 274:845-851.

Cui R, Delclos PJ, Schumer M, Rosenthal GG, 2017. Early social learning triggers neurogenomic expression changes in a swordtail fish. Proceedings of the Royal Society of London B 284. doi: 10.1098/rspb.2017.0701.

Cummings ME, Larkins-Ford J, Reilly CRL, Wong RY, Ramsey ME, Hofmann HA, 2008. Sexual and social stimuli elicit rapid and contrasting genomic repsonses. Proceedings of the Royal Society of London B 275:393-402. doi: 10.1098/rspb.2007.1454.

Datta SR, Vasconcelos ML, Ruta V, Luo S, Wong A, Demir E, Flores J, Balonze K, Dickson BJ, Axel R, 2008. The *Drosophila* pheromone cVA activates a sexually dimorphic neural circuit. Nature 452. doi: 10.1038/nature06808.

Dauwalder B, Tsujimoto S, Moss J, Mattox W, 2002. The *Drosophila* takeout gene is regulated by the somatic sex-determination pathway and affects male courtship. Genes & Development 16:2879-2892. doi: 10.1101/gad.1010302.

de Jong MA, Collins SL, Beldade P, Brakefield PM, Zwaan BJ, 2013. Footprints of selection in wild populations of *Bicyclus anynana* along a latitudinal cline. Molecular Ecology 22:341-353. doi: 10.1111/mec.12114.

Dobin A, Davis CA, Schlesinger F, Drenkow J, Zaleski C, Jha S, Batut P, Chaisson M, Gingeras TR, 2013. STAR: ultrafast universal RNA-seq aligner. Bioinformatics 29:15-21. doi: 10.1093/bioinformatics/bts635.

Edwards AC, Zwarts L, Yamamoto A, Callaerts P, Mackay TFC, 2009. Mutations in many genes affect aggressive behavior in *Drosophila melanogaster*. BMC Biology 7:29. doi: 10.1186/1741-7007-7-29.

Ehl S, Hostert K, Korsch J, Gros P, Schmitt T, 2018. Sexual dimorphism in the alpine butterflies *Boloria pales* and *Boloria napaea*: differences in movement and foraging behavior (Lepidoptera: Nymphalidae). Insect Science 25:1089-1101. doi: 10.1111/1744-7917.12494.

Ellers J, Boggs CL, 2003. The evolution of wing color: male mate choice opposes adaptive wing color divergence in *Colias* butterflies. Evolution 57:1100-1106.

Ernst DA, Westerman EL, 2021. Stage- and sex-specific transcriptome analyses reveal distinctive sensory gene expression patterns in a butterfly. BMC Genomics. doi: 10.1186/s12864-021-07819-4.

Everett A, Tong X, Briscoe AD, Monteiro A, 2012. Phenotypic plasticity in opsin expression in a butterfly compound eye complements sex role reversal. BMC Evolutionary Biology 12:232.

Ficarrotta V, Hanly JJ, Loh LS, Francescutti CM, Ren A, Tunström K, Wheat CW, Porter AH, Counterman BA, Martin A, 2022. A genetic switch for male UV-iridescence in an incipient species pair of sulpher butterflies. Proceedings of the National Academy of Sciences 119:e2109255118. doi: 10.1073/pnas.2109255118.

Ghalambor CK, Hoke KL, Ruell EW, Fischer EK, Reznick DN, Hughes KA, 2015. Non-adaptive plasticity potentiates rapid adaptive evolution of gene expression in nature. Nature 372:372-375. doi: 10.1038/nature15256.

Gobes SMH, ter Haar SM, Vignal C, Vergne AL, Mathevon N, Bolhuis JJ, 2009. Differential responsiveness in brain and behavior to sexually dimorphic long calls in male and female zebra finches. The Journal of Comparative Neurology 516:312-320. doi: 10.1002/cne.22113.

Goebrecht GKE, Kowtoniuk RA, Kelly BG, Kittelberger JM, 2014. Sexually-dimorphic expression of tyrosine hydroxylase immunoreactivity in the brain of a vocal teleost fish (*Porichthys notatus*). Journal of Chemical Neuroanatomy 56:13-34. doi: 10.1016/j.jchemneu.2014.01.001.

Greenwood PJ, 1980. Mating systems, philopatry and dispersal in birds and mammals. Animal Behaviour 28:1140-1162.

Gurney ME, Konishi M, 1980. Hormone-induced sexual differentiation of brain and behavior in zebra finches. Science 208:1380-1383.

Hashikawa K, Hashikawa Y, Lischinsky J, Lin D, 2018. The neural mechanisms of sexually dimorphic agressive behaviors. Trends in Genetics 34:755-776. doi: 10.1016/j.tig.2018.07.001.

Immelmann K, 1975. Ecological significance of imprinting and early learning. Annual Review of Ecology and Systematics 6:15-37.

Jiggins CD, Naisbit RE, Coe RL, Mallet J, 2001. Reproductive isolation caused by colour pattern mimicry. Nature 411:302-305.

Kendrick KM, Haupt MA, Hinton MR, Broad KD, Skinner JD, 2001. Sex differences in the influence of mothers on the sociosexual preferences of their offspring. Hormones and Behavior 40:322-338. doi: 10.1006/hbeh.2001.1672.

Kokko H, Johnstone RA, 2002. Why is mutual mate choice not the norm? Operational sex ratios, sex roles and the evolution of sexually dimorphic and monomorphic signalling. Philosophical transactions of the Royal Society B 357:319-330. doi: 10.1098/rstb.2001.0926.

Kronforst MR, Papa R, 2015. The functional basis of wing patterning in *Heliconius* butterflies: The molecules behind mimicry. Genetics 200:1-19. doi: 10.1534/genetics.114.172387.

Kronforst MR, Young LG, Kapan DD, McNeely C, O'Neill RJ, Gilbert LE, 2006. Linkage of butterfly mate preference and wing color preference cue at the genomic location of wingless. Proceedings of the National Academy of Sciences of the United States of America 103:6575-6580.

Kunte K, Zhang W, Tenger-Trolander A, Palmer DH, Martin A, Reed RD, Mullen SP, Kronforst MR, 2014. *doublesex* is a mimicry supergene. Nature 507:229-234. doi: 10.1038/nature13112.

Lande R, 1980. Sexual dimorphism, sexual selection, and adaptation in polygenic characters. Evolution 34:292-305.

Langfelder P, Horvath S, 2008. WGCNA: an R package for weighted correlation network analysis. BMC Bioinformatics 9:559. doi: 10.1186/1471-2105-9-559.

Lee J, Yoo E, Lee H, Park K, Hur J, Lim C, 2017. LSM12 and ME31B/DDX6 define distinct modes of posttranscriptional regulation by ATAXIN-2 protein complex in *Drosophila* circadian pacemaker neurons. Molecular Cell 66:129-140. doi: 10.1016/j.molcel.2017.03.004.

Li P, Chaurasia SS, Gao Y, Carr AL, Iuvone PM, Li L, 2008. CLOCK is required for maintaining the circadian rhythms of opsin mRNA expression in photoreceptor cells. The Journal of Biological Chemistry 283:31673-31678. doi: 10.1074/jbc.M803875200.

Li P, Temple S, Gao Y, Haimberger TJ, Hawryshyn CW, Li L, 2005. Circadian rhythms of behavioral cone sensitivity and long wavelength opsin mRNA expression: a correlation study in zebrafish. Journal of Experimental Biology 208:497-504. doi: 10.1242/jeb.01424.

London A, Benhar I, Schwartz M, 2013. The retina as a window to the brain — from eye research to CNS disorders. Nature Reviews Neurology 9:44-53. doi: 10.1038/nrneurol.2012.227.

Love MI, Huber W, Anders S, 2014. Moderated estimation of fold change and dispersion for RNA-seq data with DESeq2. Genome Biology 15:550. doi: 10.1186/s13059-014-0550-8.

Macias-Muñoz A, Smith G, Monteiro A, Briscoe AD, 2015. Transcriptome-wide differentail expression in *Bicyclus anynana* butterflies: Female vision-related genes are more plastic. Molecular Biology and Evolution. doi: 10.1093/molbev/msv197.

Martin A, Reed RD, 2010. *wingless* and *artistaless2* define a developmental ground plan for moth and butterfly wing pattern evolution. Molecular Biology and Evolution 27:2864-2878. doi: 10.1093/molbev/msq173.

Matsuoka Y, Monteiro A, 2018. Melanin pathway genes regulate color and morphology of butterfly wing scales. Cell Reports 24:56-65. doi: 10.1016/j.celrep.2018.05.092.

Merrill RM, Dasmahapatra KK, Davey JW, Dell'Aglio DD, Hanly JJ, Huber B, Jiggins CD, Joron M, Kozak KM, Llaurens V, Marin SH, Montgomery SH, Morris J, Nadeau NJ, Pinharanda AL, Rosser N, Thompson MJ, Vanjari S, Wallbank RWR, Yu Q, 2015. The diversification of *Heliconius* butterflies: what have we learned in 150 years? Journal of Evolutionary Biology 28:1417-1438. doi: 10.1111/jeb.12672.

Merrill RM, Rastas P, Martin SH, Melo MC, Barker S, Davey JW, McMillan WO, Jiggins CD, 2019. Genetic dissection of assortative mating behavior. PLoS Biology 17:e2005902. doi: 10.1371/journal.pbio.2005902.

Monteiro A, Chen B, Ramos DM, Oliver JC, Tong X, Guo M, Wang W, Fazzino L, Kamal F, 2013. Distal-Less regulates eyespot patterns and melanization in *Bicyclus* butterflies. Journal of Experimental Zoology Part B 320B:321-331.

Monteiro A, Glaser G, Stockslager S, Glansdorp N, Ramos D, 2006. Comparative insights into questions of lepidopteran wing pattern homology. BMC Developmental Biology 6:52. doi: 10.1186/1471-213X-6-52.

Monteiro A, Prudic KL, 2010. Multiple approaches to study color pattern evolution in butterflies. Trends in Evolutionary Biology 2. doi: 10.4081/eb.2010.e2.

Morandin C, Hietala A, Helanterä H, 2019. Vitellogenin and vitellogenin-like gene expression patterns in relation to caste and task in the ant *Formica fusca*. Insectes Sociaux 66:519-531. doi: 10.1007/s00040-019-00725-9.

Nadeau NJ, Pardo-Diaz C, Whibley A, Supple MA, Saenko SV, Wallbank RWR, Wu GC, Maroja L, Ferguson L, Hanly JJ, Hines H, Salazar C, Merrill RM, Dowling AJ, ffrench-Constant RH, Llaurens V, Joron M, McMillan WO, Jiggins CD, 2016. The gene *cortex* controls mimicry and crypsis in butterflies and moths. Nature 534:106-110. doi: 10.1038/nature17961.

Naisbit RE, Jiggins CD, Mallet J, 2001. Disruptive sexual selection against hybrids contributes to speciation between *Heliconius cydno* and *Heliconius melpomene*. Proceedings of the Royal Society of London B 268:1849-1854. doi: 10.1098/rspb.2001.1753.

Nelson CM, Ihle KE, Fondrk MK, Page RE, Amdam GV, 2007. The gene *vitellogenin* has multiple coordinating effects on social organization. PLoS Biology 5:e62. doi: 10.1371/journal.pbio.0050062.

Nieberding CM, de Vos H, Schneider MV, Lassance J, Estramil N, Andersson J, Bang J, Hedenstrom E, Lofstedt C, Brakefield PM, 2008. The male sex pheromone of the butterfly *Bicyclus anynana*: Towards an evolutionary analysis. PLoS ONE 3:e2751-.

Nieberding CM, Fischer K, Saastamoinen M, Allen CE, Wallin EA, Hedenstrom E, Brakefield PM, 2012. Cracking the olfactory code of a butterfly: the scent of ageing. Ecology Letters 15:415-424. doi: 10.1111/j.1461-0248.2012.01748.x.

Nowell RW, Elsworth B, V. O, Zwaan BJ, Wheat CW, Saastamoinen M, Saccheri IJ, van't Hof AE, Wasik BR, Connahs H, Aslam ML, Kumar S, challis RJ, Monteiro A, Brakefield PM, Blaxter ML, 2017. A high-coverage draft genome of the mycalesine butterfly *Bicyclus anynana*. Giga Science 6:1-7. doi: 10.1093/gigascience/gix035.

Obara Y, Koshitaka H, Arikawa K, 2008. Better mate in the shade: enhancement of male mating behavior in the cabbage butterfly, *Pieris rapae crucivora*, in a UV-rich environment. Journal of Experimental Biology 211:3698-3702.

Ogawa Y, Kinoshita M, Stavenga DG, Arikawa K, 2013. Sex-specific retinal pigmentation results in sexually dimorphic long-wavelength-sensitive photoreceptors in the eastern pale clouded yellow butterfly, *Colias erate*. The Journal of Experimenbtal Biology 216:1916-1923. doi: 10.1242/jeb.083485.

Olson CR, Hodges LK, Mello CV, 2015. Dynamic gene expression in the song system of zebra finches during the song learing period. Developmental Neurobiology 75:1315-1338. doi: 10.1002/dneu.2286.

Ozsu N, Chan QY, Chen B, Das Gupta M, Monteiro A, 2017. *Wingless* is a positive regulator of eyespot color patterns in *Bicyclus anynana* butterflies. Developmental Biology 429:177-185. doi: 10.1016/j.ydbio.2017.06.030.

Ozsu N, Monteiro A, 2017. Wound healing, calcium signaling, and other novel pathways are associated with the formation of butterfly eyespots. BMC Genomics 18:788. doi: 10.1186/s12864-017-4175-7.

Perry CJ, Barron AB, Chittka L, 2017. The frontiers of insect cognition. Current Opinion in Behavioral Sciences 16:111-118. doi: 10.1016/j.cobeha.2017.05.011.

Pradhan A, Olsson P, 2015. Zebrafish sexual behavior: role of sex steroid hormones and prostaglandins. Behavioral and Brain Functions 11:23. doi: 10.1186/s12993-015-0068-6.

Prakash A, Monteiro A, 2018. *apterous A* specifies dorsal wing patterns and sexual traits in butterflies. Proceedings of the Royal Society of London B 285:20172685. doi: 10.1098/rspb.2017.2685.

Prakash A, Monteiro A, 2020. *Doublesex* mediates the development of sex-specific pheromone organs in *Bicyclus* butterflies via multiple mechanisms. Molecular Biology and Evolution 37:1694-1707. doi: 10.1093/molbev/msaa039.

Prudic KL, Jeon C, Cao H, Monteiro A, 2011. Developmental plasticity in sexual roles of butterfly species drives mutual sexual ornamentation. Science 331:73-75. doi: 10.1126/science.1197114.

Quillfeldt P, Schroff S, van Noordwijk HJ, Michalik A, Ludynia K, Masello JF, 2011. Felxible foraging behaviour of a sexually dimorphic seabird: large males do not always dive deep. Marine Ecology Progress Series 428:271-287. doi: 10.3354/meps09058.

Reed RD, Papa R, Martin A, Hines HM, Counterman BA, Pardo-Diaz C, Jiggins CD, Chamberlain NL, Kronforst MR, Chen R, Halder G, Nijhout HF, McMillan WO, 2011. *optix* drives the repeated convergent evolution of butterfly wing pattern mimcry. Science 333:1137-1141. doi: 10.1126/science.1208227.

Reedy AM, Pope BD, Kiriazis NM, Giordano CL, Sams CL, Warner DA, Cox RM, 2017. Female anoles display less but attack more quickly than males in response to territorial intrusions. Behavioral Ecology 28:1323-1328. doi: 10.1093/beheco/arx095.

Rideout EJ, Billeter J, Goodwin SF, 2007. The sex-determination genes *fruitless* and *doublesex* specify a neural substrate required for courtship song. Current Biology 17:1473-1478. doi: 10.1016/j.cub.2007.07.047.

Robertson KA, Monteiro A, 2005. Female *Bicyclus anynana* butterflies choose males on the basis of their dorsl UV-reflectve eyespot pupils. Proceedings of the Royal Society of London B 272:1541-1546.

Robinson MD, McCarthy DJ, Smyth GK, 2010. edgeR: a Bioconductor package for differential expression analysis of digital gene expression data. Bioinformatics 26:139-140. doi: 10.1093/bioinformatics/btp616.

Rodriguez-Caro F, Fenner J, Bhardwayj S, Cole JA, Benson C, Colombara AM, Papa R, Brown MW, Martin A, Range RC, Counterman BA, 2021. Novel *doublesex* duplication associated with sexually dimorphic development of dogface butterfly wings. Molecular Biology and Evolution 38:5021-5033. doi: 10.1093/molbev/msab228.

Rosell F, Thomsen LR, 2006. Sexual dimorphism in territorial scent marking by adult Eurasian beavers (*Castor fiber*). Journal of Chemical Ecology 32:1301-1315. doi: 10.1007/s10886-006-9087-y.

Roy-Zokan EM, Cunningham CB, Hebb LE, McKinney EC, Moore AJ, 2015. Vitellogenin and vitellogenin receptor gene expression is associated with male and female parenting in a subsocial insect. Proceedings of the Royal Society of London B 282:20150787. doi: 10.1098/rspb.2015.0787.

Rue-Albrecht K, McGettigan PA, Hernández B, Nalpas NC, Magee DA, A.C. P, Gordon SV, MacHugh DE, 2016. GOexpress: an R/Bioconductor package for the identification and visualisation of robust gene ontology signatures through supervised learning of gene expression data. BMC Bioinformatics 17:126. doi: 10.1186/s12859-016-0971-3.

Ruta V, Datta SR, Vasconcelos ML, Freeland J, Looger LL, Axel R, 2010. A dimorphic pheromone circuit in *Drosophila* from sensory input to descending output. Nature 468:686-692. doi: 10.1038/nature09554.

Saenko SV, Marialva MSP, Beldade P, 2011. Involvement of the conserved Hox gene *Antennapedia* in the development and evolution of a novel trait. EvoDevo 2:9. doi: 10.1186/2041-9139-2-9.

Sakai Y, Kawamura S, Kawata M, 2018. Genetic and plastic variation in opsin gene expression, light sensitivity, and female response to visual signals in the guppy. Proceedings of the National Academy of Sciences 115:12247-12252. doi: 10.1073/pnas.1706730115.

Schwaerzel M, Monastirioti M, Scholz H, Friggi-Grelin F, Birman S, Heisenberg M, 2003. Dopamine and octopamine differentiate between aversive and appetitive olfactory memories in *Drosophila*. Journal of Neuroscience 23:10495-10502.

Servedio MR, 2009. The role of linkage disequilibrium in the evolution of premating isolation. Heredity 102:51-56. doi: 10.1038/hdy.2008.98.

Servedio MR, Van Doorn GS, Kopp M, Frame AM, Nosil P, 2011. Magic traits in speciation: 'magic' but not rare? Trends in Ecology & Evolution 26:389-397. doi: 10.1016/j.tree.2011.04.005.

Shannon G, Page BR, Duffy KJ, Slotow R, 2006. The role of foraging behaviour in the sexual segregation of the African elephant. Oecologia 150:344-354. doi: 10.1007/s00442-006-0521-1.

Shannon P, Markiel A, Ozier O, Baliga NS, Wang JT, Ramage D, Amin N, Schwikowski B, Ideker T, 2003. Cytoscape: a software environment for integrated models of biomolecular interaction networks. Genome Research 13:2498-2504.

Slonim DK, 2002. From patterns to pathways: gene expression data analysis comes of age. Nature Genetics 32:502-508. doi: 10.1038/ng1033.

Smadja CM, Butlin RK, 2011. A framework for comparing processes of speciation in the presence of gene flow. Molecular Ecology 20:5123-5140. doi: 10.1111/j.1365-294X.2011.05350.x.

Stavenga DG, 2002. Reflections on colourful ommatidia of butterfly eyes. Journal of Experimental Biology 205:1077-1085.

Stephens M, 2017. False discovery rates: a new deal. Biostatistics 18:275-294. doi: 10.1093/biostatistics/kxw041.

Talyn BC, Dowse HB, 2004. The role of courtship song in sexual selection and species recognition by female *Drosophila melanogaster*. Animal Behaviour 68:1165-1180. doi: 10.1016/j.anbehav.2003.11.023.

ten Cate C, 1985. On sex differences in sexual imprinting. Animal Behaviour 33:1310-1317.

ten Cate C, Vos DR, 1999. Sexual imprinting and evolutionary processes in birds: a reassessment. Advances in the Study of Behavior 28:1-31.

Trivers RL, 1972. Parental investment and sexual selection. In: Campbell B, editor. Sexual Selection and the Descent of Man, 1871-1971 Chicago: Aldine-Atherton. p. 136-179.

Trochet A, Courtois EA, Stevens VM, Baguette M, Chaine A, Schmeller DS, Clobert J, 2016. Evolution of sex-biased dispersal. The Quarterly Review of Biology 91:297-320.

van Schooten B, Meléndez-Rosa J, Van Belleghem SM, Jiggins CD, Tan JD, McMillan WO, Papa R, 2020. Divergence of chemosensing during the early stages of speciation. Proceedings of the National Academy of Sciences 117:16438-16447. doi: 10.1073/pnas.1921318117.

Verzijden MN, Korthof REM, ten Cate C, 2008. Females learn from mothers and males learn from others. The effect of mother and siblings on the development of female mate preferences and male aggression biases in Lake Vicotria cichlids, genus Mbipia. Behavioral Ecology and Sociobiology 62:1359-1368. doi: 10.1007/s00265-008-0564-x.

Verzijden MN, ten Cate C, Servedio MR, Kozak GM, Boughman JW, Svensson EI, 2012. The impact of learning on sexual selection. Trends in Ecology and Evolution 27:511-519. doi: 10.1016/j.tree.2012.05.007.

Wang Y, Rensink A, Fricke U, Riddle MC, Trent C, van de Zande L, Verhulst EC, 2022. *Doublesex* regulates male-specific differentiation during distinct developmental time windows in a parasitoid wasp. Insect Biochemistry and Molecular Biology 142:103724. doi: 10.1016/j.ibmb.2022.103724.

Westerman E, 2019. Searching for the genes driving assortative mating. PLoS Biology 17:e3000108. doi: 10.1371/journal.pbio.3000108.

Westerman E, Hodgins-Davis A, Dinwiddie A, Monteiro A, 2012. Biased learning affects mate choice in a butterfly. Proceedings of the National Academy of Sciences of the United States of America 109:10948-10953. doi: 10.1073/pnas.1118378109.

Westerman E, Monteiro A, 2013. Odour influences whether females learn to prefer or to avoid wing patterns of male butterflies. Animal Behaviour 86:1139-1145. doi: 10.1016/j.anbehav.2013.09.002.

Westerman EL, Antonson N, Kreutzmann S, Peterson A, Pineda S, Kronforst MR, Olson-Manning CF, 2019. Behaviour before beauty: Signal weighting during mate selection in the butterfly *Papilio polytes*. Ethology 125:565-574. doi: 10.1111/eth.12884.

Westerman EL, Chirathivat N, Schyling E, Monteiro A, 2014. Mate preference for a phenotypically plastic trait is learned, and may facilitate preference-phenotype matching. Evolution 68:1661-1670.

Westerman EL, VanKuren N, Massardo D, Buerkle N, Tenger-Trolander A, Zhang W, Hill R, Perry M, Bayala E, Chamberlain N, Douglas T, Palmer S, Kronforst MR,

2018. *Aristaless* controls butterfly wing color variation used in mimicry and mate choice. Current Biology 28:3469-3474.e3464. doi: 10.1016/j.cub.2018.051.
Witte K, Sawka N, 2003. Sexual imprinting on a novel trait in the dimorphic zebra finch: sexes differ. Animal Behaviour 65:165-203. doi: 10.1006/anbe.2002.2009.
Wong BBM, Fisher HS, Rosenthal GG, 2005. Species recognition by male swordtails via chemical cues. Behavioral Ecology 16:818-822. doi: 10.1093/beheco/ari058.
Woodgate JL, Buchanan KL, Bennett ATD, Catchpole CK, Birghton R, Leitner S, 2014. Environmental and genetic control of brain and song structure in the zebra finch. Evolution 68:230-240. doi: 10.1111/evo.12261.
Woronik A, Tunström K, Perry MW, Neethiraj R, Stefanescu C, Celorio-Mancera M, Brattstrom O, Hill J, Lehmann P, Käkelä R, Wheat CW, 2019. A transposable element insertion is associated with an alternative life history strategy. Nature Communications 10:5757. doi: 10.1038/s41467-019-13596-2.
Wright DS, van Eijk R, Schuart L, Seehausen O, Groothuis TGG, Maan ME, 2020. Testing sensory drive speciation in cichlid fish: linking light conditions to opsin expression, opsin genotype and female mate preference. Journal of Evolutionary Biology 33:422-434. doi: 10.1111/jeb.13577.
Zhou X, Pardue MT, Iuvone PM, Qu J, 2017. Dopamine signaling and myopia development: What are the key challenges. Progress in Retinal and Eye Research 61:60-71. doi: 10.1016/j.preteyeres.2017.06.003.
Zilkha N, Scott N, Kimchi T, 2017. Sexual dimorphism of parental care: from genes to behavior. Annual Review of Neuroscience 40:273-305. doi: 10.1146/annurev-neuro-072116-031447.

Data Availability Statement: All raw sequence data associated with this study are accessible through the NCBI Sequence Read Archive (SRA) database under BioProject ID PRJNA935913. Behavioral data are available at Dryad Database DOI: 10.5061/dryad.612jm647d. All other data presented in this study and associated metadata are available within this manuscript and its Supplemental Information.

Benefits Generated: Benefits from this research accrue from the sharing of our data and results on public databases as described above.

Author Contributions: DAE- conceptualization, investigation, methodology, data curation, formal analysis, visualization, writing- original draft, review & editing; GAA-

conceptualization, investigation, formal analysis, writing-original draft, review & editing; ANM- formal analysis, visualization, writing-original draft, review & editing; ELW-conceptualization, investigation, methodology, resources, visualization, writing-original draft, review & editing

Figures

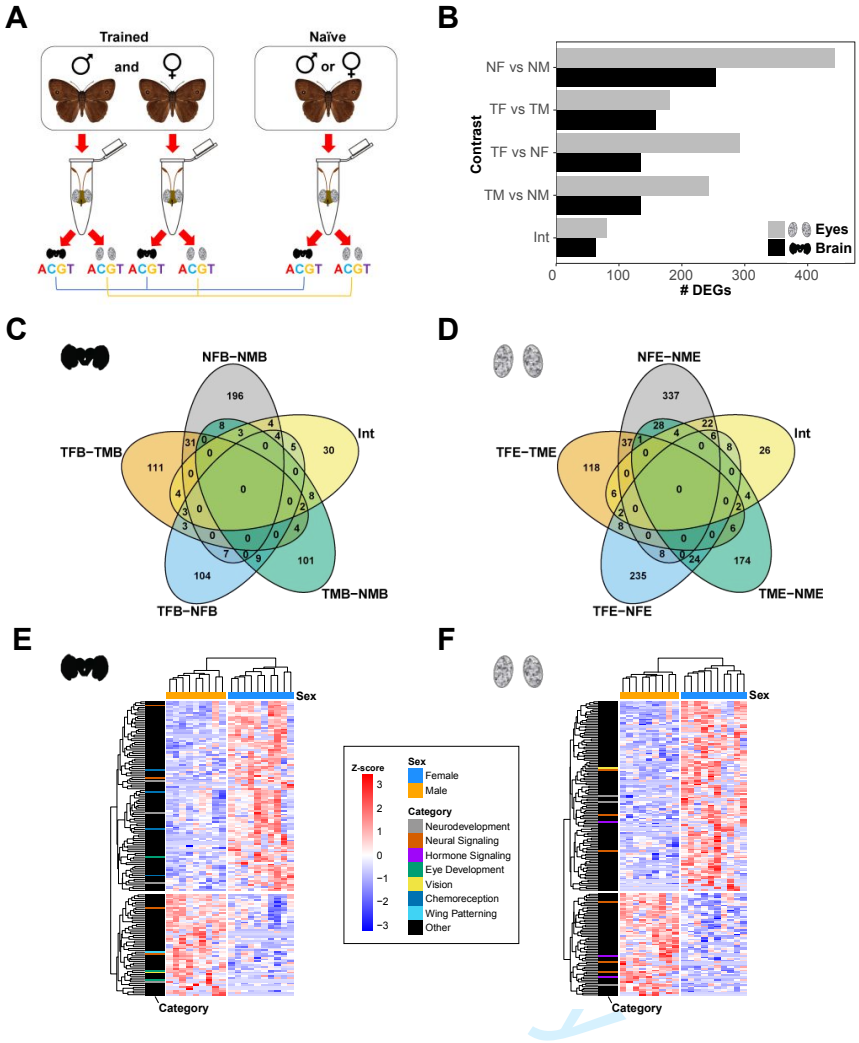

Figure 1: Experimental design and broadscale sexually dimorphic gene expression. A) Protocol for butterfly training and sampling. Newly emerged males/females were either solo or paired with a two-day-old, zero-spot female/four-spot male. Heads of each focal animal were collected, the brain and eyes dissected, and mRNA sequenced for expression analysis. B) Numbers of differentially expressed genes for each comparison for each tissue. C) Brain Venn diagrams showing overlap patterns for differentially expressed genes. D) Eye Venn diagrams showing overlap patterns for differentially expressed genes. E) Brain gene expression heatmaps of differentially expressed genes from trained females vs. trained males. Each row indicates a single gene, and each column indicates an individual sample. Counts were first normalized by variance stabilizing transformation, and gene-wise Z-scores were calculated for plotting. Genes and samples are clustered by expression, with warmer colors denoting increased expression relative to the mean for a given gene, while cooler colors denote decreased expression relative to

the mean. F) Eye gene expression heatmaps of differentially expressed genes from trained females vs. trained males. NFB=naïve female brain, NMB=naïve male brain, TFB=trained female brain, TMB=trained male brain, NFE=naïve female eye, NME=naïve male eye, TFE=trained female eye, TME=trained male eye, Int=interaction.

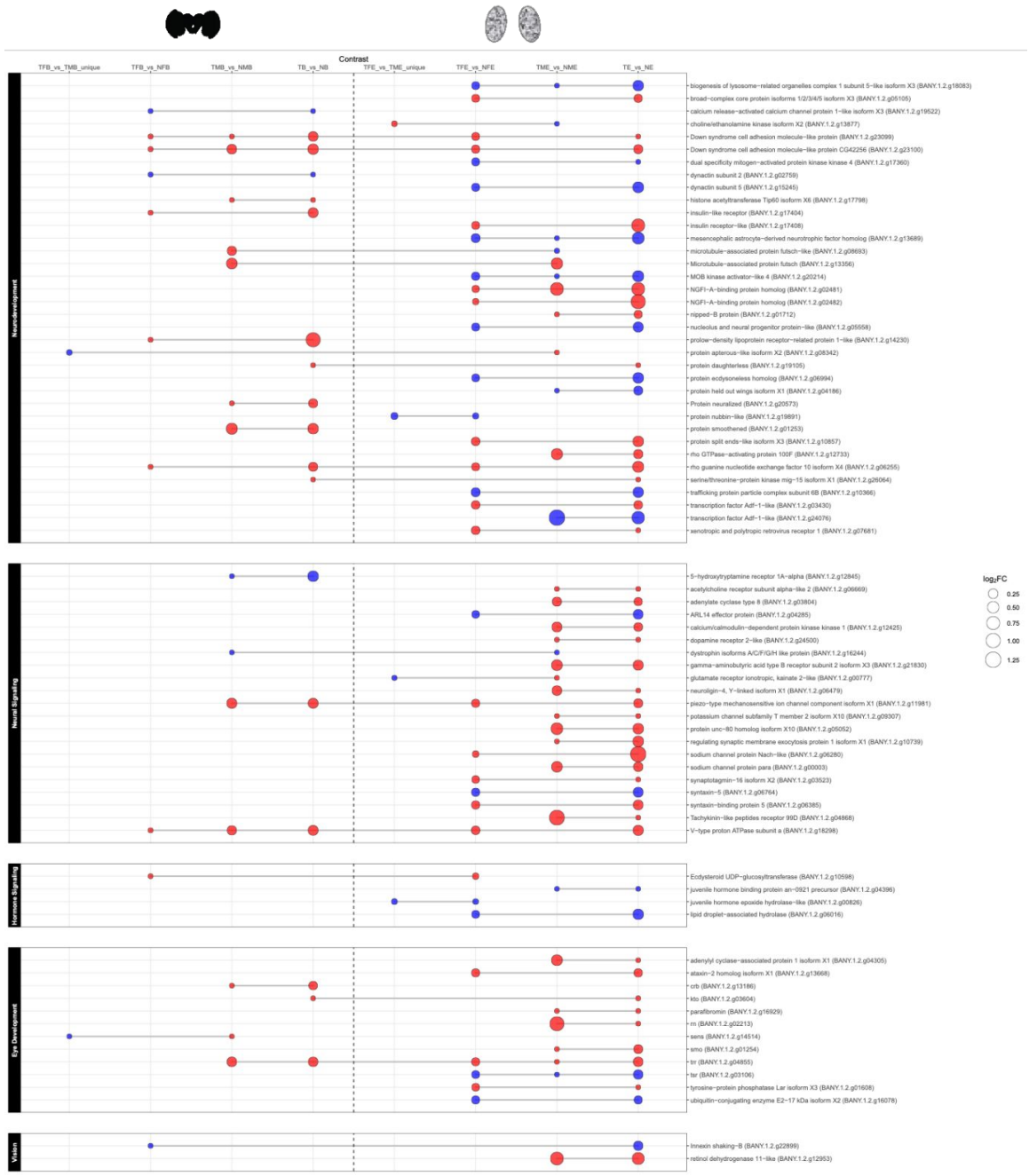
Contrast
TFB_vs_TMB_unique
TFB_vs_NFB
TMB_vs_NMB
TB_vs_NB
TFE_vs_TME_unique
TFE_vs_NFE
TME_vs_NME
TE_vs_NE
Neurodevelopment
biogenesis of lysosome-related organelles complex 1 subunit 5-like isoform X3 (BANY.1.2.g18083)
broad-complex core protein isoforms 1/2/3/4/5 isoform X3 (BANY.1.2.g05105)
calcium release-activated calcium channel protein 1-like isoform X3 (BANY.1.2.g19522)
choline/ethanolamine kinase isoform X2 (BANY.1.2.g13877)
Down syndrome cell adhesion molecule-like protein (BANY.1.2.g23099)
Down syndrome cell adhesion molecule-like protein CG42256 (BANY.1.2.g23100)
dual specificity mitogen-activated protein kinase kinase 4 (BANY.1.2.g17360)
dynactin subunit 2 (BANY.1.2.g02759)
dynactin subunit 5 (BANY.1.2.g15245)
histone acetyltransferase Tip60 isoform X6 (BANY.1.2.g17798)
insulin-like receptor (BANY.1.2.g17404)
insulin receptor-like (BANY.1.2.g17408)
mesencephalic astrocyte-derived neurotrophic factor homolog (BANY.1.2.g13689)
microtubule-associated protein futsch-like (BANY.1.2.g08693)
Microtubule-associated protein futsch (BANY.1.2.g13356)
MOB kinase activator-like 4 (BANY.1.2.g20214)
NGFI-A-binding protein homolog (BANY.1.2.g02481)
NGFI-A-binding protein homolog (BANY.1.2.g02482)
nipped-B protein (BANY.1.2.g01712)
nucleolus and neural progenitor protein-like (BANY.1.2.g05558)
prolow-density lipoprotein receptor-related protein 1-like (BANY.1.2.g14230)
protein apterous-like isoform X2 (BANY.1.2.g08342)
protein daughterless (BANY.1.2.g19105)
protein ecdysoneless homolog (BANY.1.2.g06994)
protein held out wings isoform X1 (BANY.1.2.g04186)
Protein neuralized (BANY.1.2.g20573)
protein nubbin-like (BANY.1.2.g19891)
protein smoothened (BANY.1.2.g01253)
protein split ends-like isoform X3 (BANY.1.2.g10857)
rho GTPase-activating protein 100F (BANY.1.2.g12733)
rho guanine nucleotide exchange factor 10 isoform X4 (BANY.1.2.g06255)
serine/threonine-protein kinase mig-15 isoform X1 (BANY.1.2.g26064)
trafficking protein particle complex subunit 6B (BANY.1.2.g10366)
transcription factor Adf-1-like (BANY.1.2.g03430)
transcription factor Adf-1-like (BANY.1.2.g24076)
xenotropic and polytropic retrovirus receptor 1 (BANY.1.2.g07681)
Neural Signaling
5-hydroxytryptamine receptor 1A-alpha (BANY.1.2.g12845)
acetylcholine receptor subunit alpha-like 2 (BANY.1.2.g06669)
adenylate cyclase type 8 (BANY.1.2.g03804)
ARL14 effector protein (BANY.1.2.g04285)
calcium/calmodulin-dependent protein kinase kinase 1 (BANY.1.2.g12425)
dopamine receptor 2-like (BANY.1.2.g24500)
dystrophin isoforms A/C/F/G/H like protein (BANY.1.2.g16244)
gamma-aminobutyric acid type B receptor subunit 2 isoform X3 (BANY.1.2.g21830)
glutamate receptor ionotropic, kainate 2-like (BANY.1.2.g00777)
neuroligin-4, Y-linked isoform X1 (BANY.1.2.g06479)
piezo-type mechanosensitive ion channel component isoform X1 (BANY.1.2.g11981)
potassium channel subfamily T member 2 isoform X10 (BANY.1.2.g09307)
protein unc-80 homolog isoform X10 (BANY.1.2.g05052)
regulating synaptic membrane exocytosis protein 1 isoform X1 (BANY.1.2.g10739)
sodium channel protein Nach-like (BANY.1.2.g06280)
sodium channel protein para (BANY.1.2.g00003)
synaptotagmin-16 isoform X2 (BANY.1.2.g03523)
syntaxin-5 (BANY.1.2.g06764)
syntaxin-binding protein 5 (BANY.1.2.g06385)
Tachykinin-like peptides receptor 99D (BANY.1.2.g04868)
V-type proton ATPase subunit a (BANY.1.2.g16298)
log2FC
0.25
0.50
0.75
1.00
1.25
Hormone Signaling
Ecdysteroid UDP-glucosyltransferase (BANY.1.2.g10598)
juvenile hormone binding protein an-0921 precursor (BANY.1.2.g04396)
juvenile hormone epoxide hydrolase-like (BANY.1.2.g00826)
lipid droplet-associated hydrolase (BANY.1.2.g06016)
Eye Development
adenylyl cyclase-associated protein 1 isoform X1 (BANY.1.2.g04305)
ataxin-2 homolog isoform X1 (BANY.1.2.g13668)
crb (BANY.1.2.g13186)
ldo (BANY.1.2.g03604)
parafibromin (BANY.1.2.g16929)
rn (BANY.1.2.g02213)
sens (BANY.1.2.g14514)
smo (BANY.1.2.g01254)
trr (BANY.1.2.g04855)
tsr (BANY.1.2.g03106)
tyrosine-protein phosphatase Lar isoform X3 (BANY.1.2.g01608)
ubiquitin-conjugating enzyme E2-17 kDa isoform X2 (BANY.1.2.g16078)
Vision
Innexin shaking-B (BANY.1.2.g22899)
retinol dehydrogenase 11-like (BANY.1.2.g12953)

Figure 2: Neural processing, hormone signaling, and vision genes are differentially expressed in multiple contrasts. The size of each dot indicates the effect size (log_2FC), while the color indicates the gene regulation relative to the first sample type listed for the contrast (e.g., for the TB vs. NB contrast, red indicates upregulation in trained brains, and blue indicates downregulation in trained brains). Gray lines connecting the dots denote that the gene was differentially expressed across multiple contrasts. NFB=naïve female brain, NMB=naïve male brain, TFB=trained female brain, TMB=trained male brain, NFE=naïve female eye, NME=naïve male eye, TFE=trained female eye, TME=trained male eye, TB=trained brain, TE=trained eye, NB=naïve brain, NE=naïve eye.

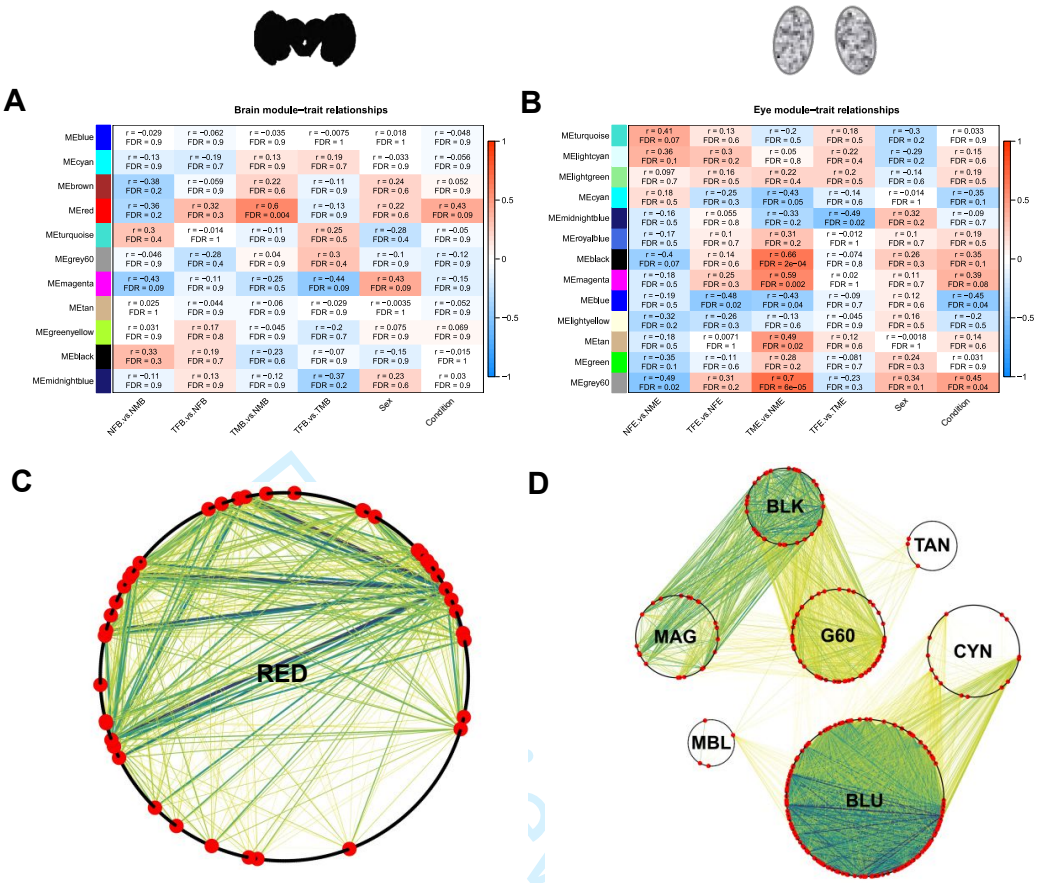

Figure 3: Gene network modules in brain and eyes are significantly associated with training. Significant modules from co-expression analyses. A) Brain module-trait association heatmap. Rows indicate module eigengenes (ME), and columns indicate the pairwise binary indicators representing the various comparisons ("traits") of interest. The top numbers in each cell denote the correlation value (r), with false discovery rate (FDR) values below. Cells are colored by the strength of the association, with r ranging from -1 to 1. B) Eye module-trait association heatmap. C) WGCNA brain analysis red module Cytoscape plot. Each black dot around the perimeter of the circle indicates a node (gene), with larger red dots indicating differentially expressed genes from the contrast for which the module is significantly associated (i.e., trained vs. naïve male brain). Each line indicates an edge (connection) for differentially expressed genes within the module, with thinner yellow lines indicating weaker connections and thicker blue lines indicating stronger connections. D) WGCNA eye analysis, Cytoscape plot of all significant modules. Only edges for differentially expressed genes within and between modules are shown. BLK=black module, BLU=blue module, CYN=cyan module, G60=grey60 module, MAG=magenta module, MBL=midnightblue module, RED=red module, and TAN=tan module.

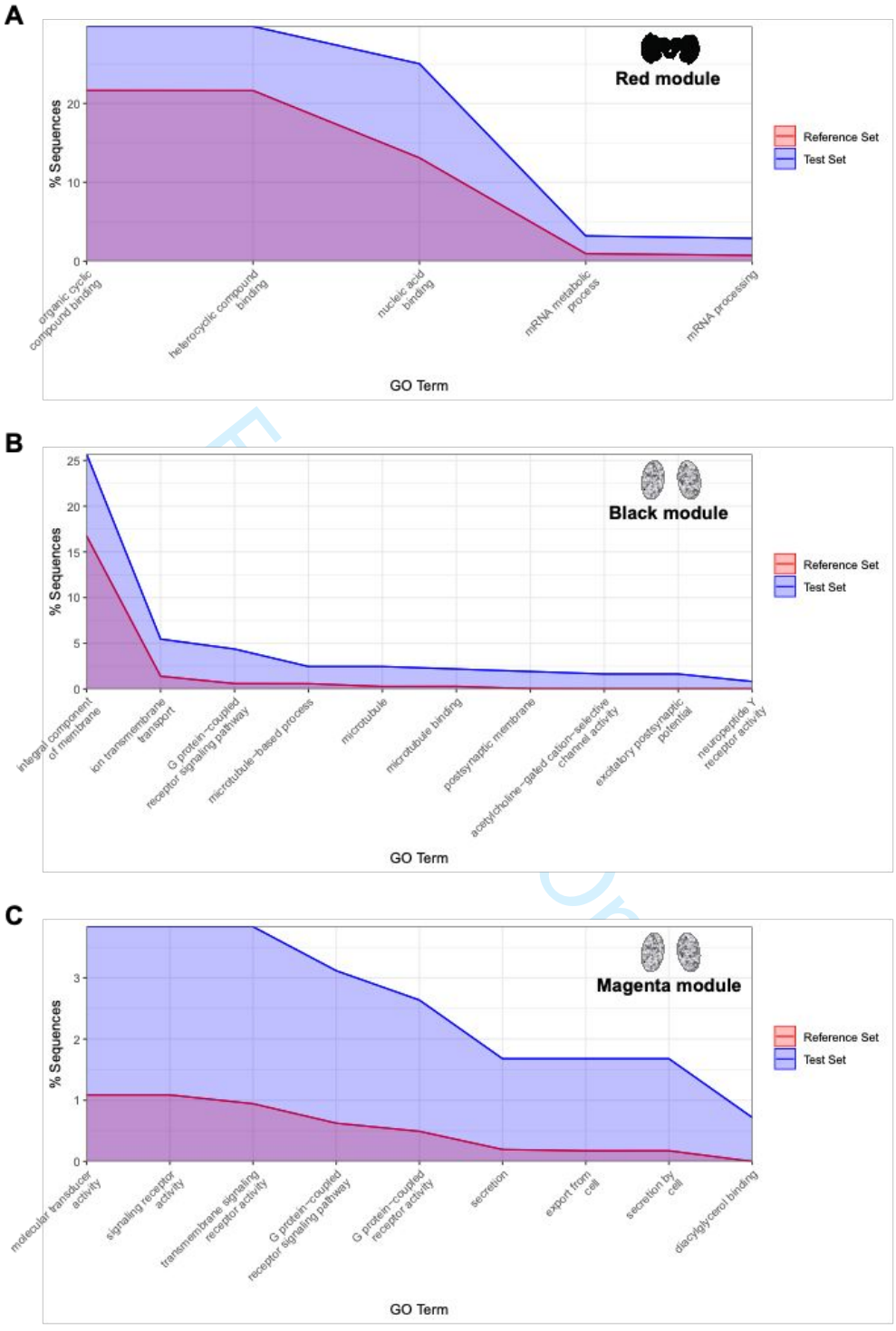

Figure 4: Gene ontology enrichment plots for significant brain and eye modules of interest. A) Significantly enriched GO terms in the brain red module. For each GO term, the percentage of sequences annotated with that term within the Test Set (i.e., all red module genes) is plotted along

with the percentage of sequences annotated with that term within the Reference Set (i.e., all genes used in the co-expression analysis). B) Significantly enriched GO terms in the eye black module. Due to the large number of enriched GO terms in this module, only the most specific terms identified by Blast2GO were plotted for clarity. C) Significantly enriched GO terms in the eye magenta module.

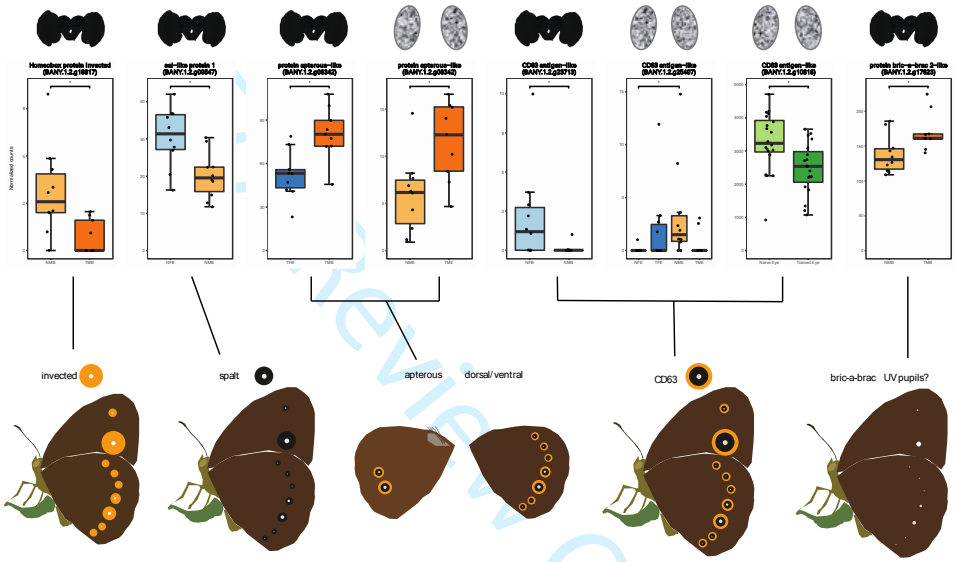

Figure 5: **Genes that influence *B. anynana* wing patterns are also differentially expressed in the brain and eye during training.** Top panel contains box plots of differentially expressed genes in different contrasts. Bottom panel indicates the elements of butterfly wing pattern (gold ring, eye spot center, black ring, whole eye spot, or dorsal/ventral identity) influenced by the corresponding differentially expressed gene. For top panel, light hue = naïve, dark hue = trained, orange = male, blue = female, green = condition (general trained/naïve). Asterisks indicate FDR<0.05. Dark horizontal lines inside boxes indicate median with upper and lower box bounds denoting the 25th and 75th percentiles. The box whiskers denote the largest and smallest count values ≤1.5× the interquartile range.

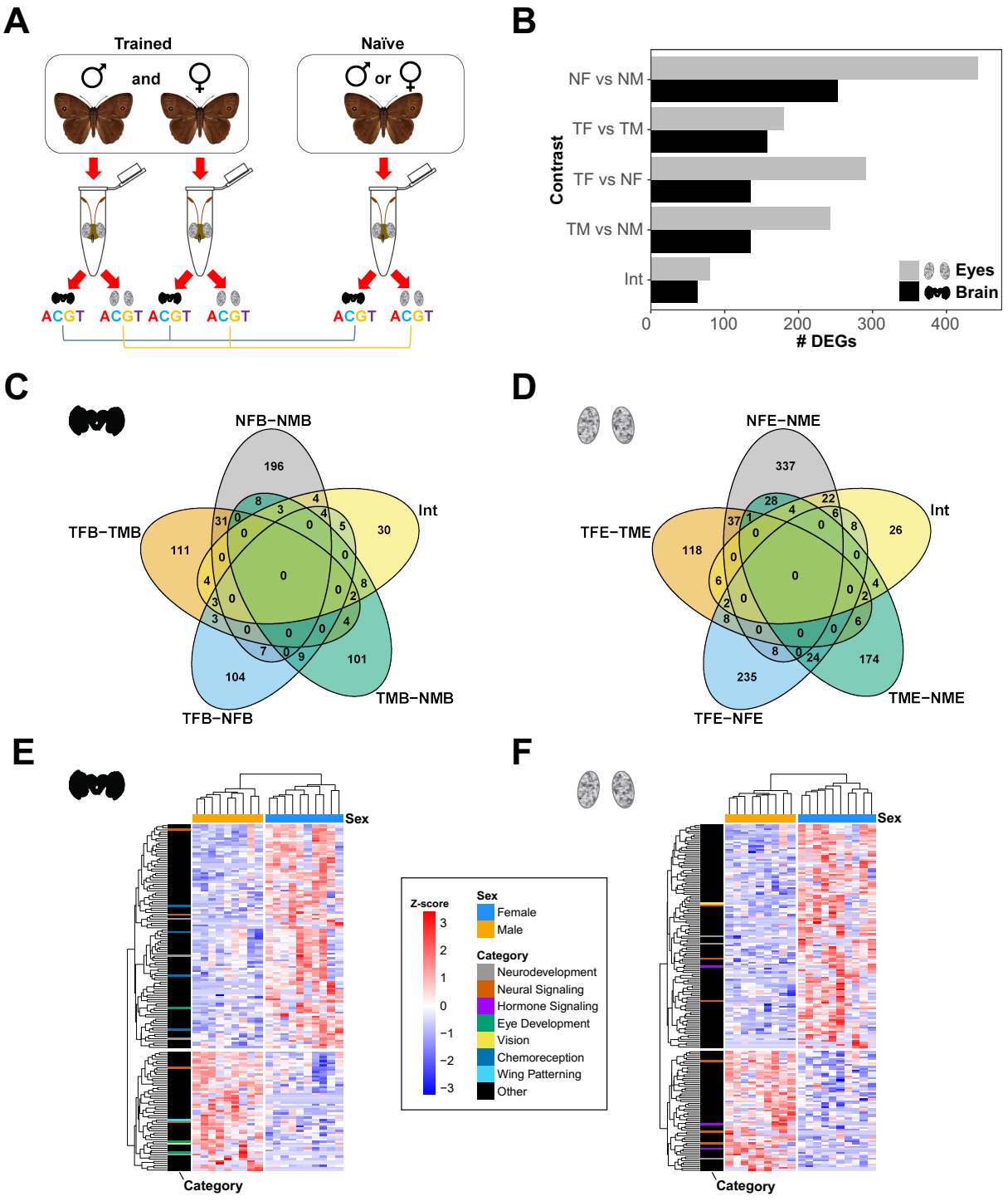
A
Trained
Naïve
and
or
ACGT
B
NF vs NM
TF vs TM
TF vs NF
TM vs NM
Int
Contrast
Eyes
Brain
0
100
200
300
400
DEGs
C
NFB−NMB
TFB−TMB
Int
TMB−NMB
TFB−NFB
196
111
30
101
104
D
NFE−NME
TFE−TME
Int
TME−NME
TFE−NFE
337
118
26
174
235
E
Sex
Category
F
Sex
Category
Z-score
3
2
1
0
−1
−2
−3
Sex
Female
Male
Category
Neurodevelopment
Neural Signaling
Hormone Signaling
Eye Development
Vision
Chemoreception
Wing Patterning
Other

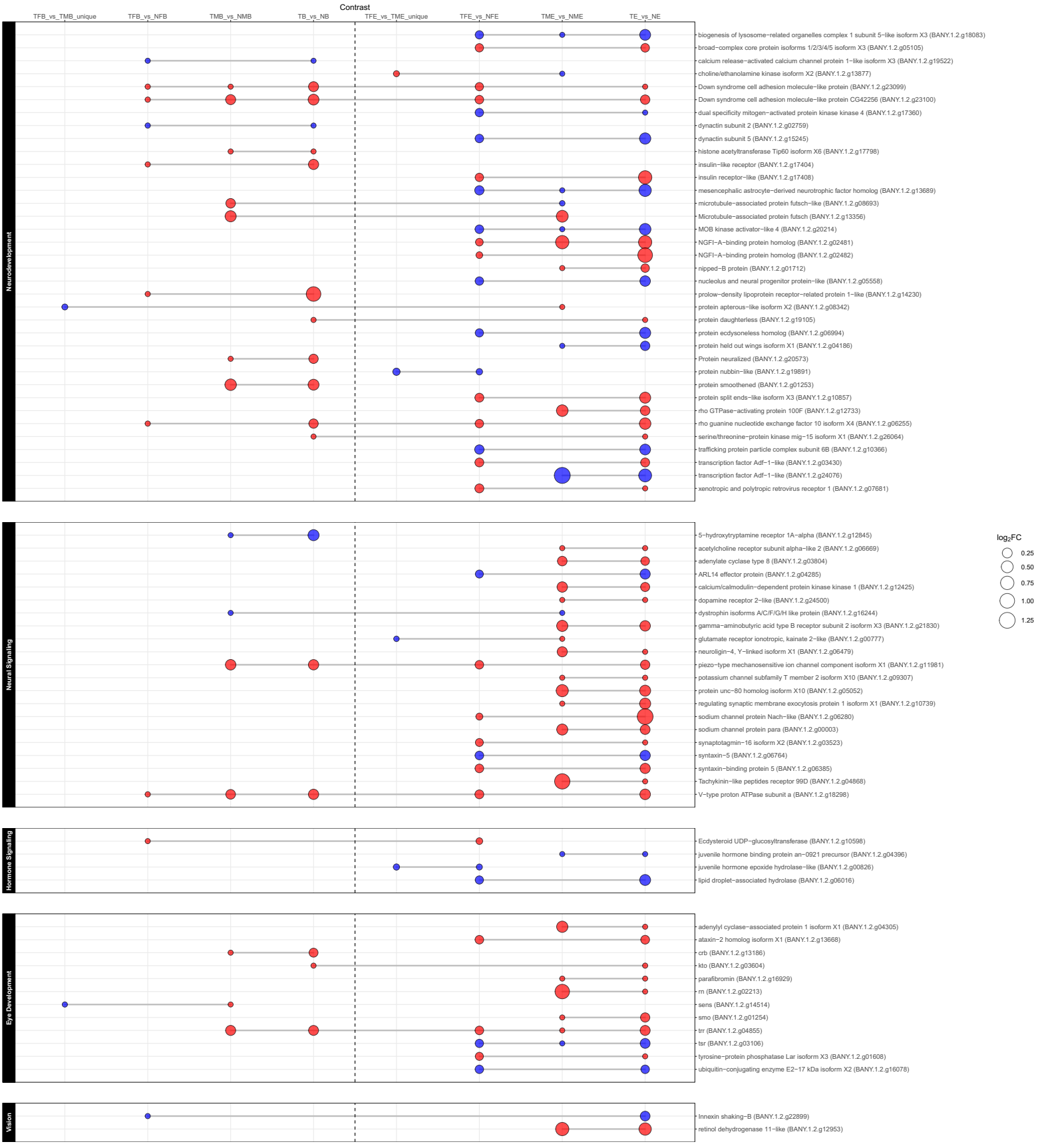
Contrast
TFB_vs_TMB_unique
TFB_vs_NFB
TMB_vs_NMB
TB_vs_NB
TFE_vs_TME_unique
TFE_vs_NFE
TME_vs_NME
TE_vs_NE
Neurodevelopment
biogenesis of lysosome-related organelles complex 1 subunit 5-like isoform X3 (BANY.1.2.g18083)
broad-complex core protein isoforms 1/2/3/4/5 isoform X3 (BANY.1.2.g05105)
calcium release-activated calcium channel protein 1-like isoform X3 (BANY.1.2.g19522)
choline/ethanolamine kinase isoform X2 (BANY.1.2.g13877)
Down syndrome cell adhesion molecule-like protein (BANY.1.2.g23099)
Down syndrome cell adhesion molecule-like protein CG42256 (BANY.1.2.g23100)
dual specificity mitogen-activated protein kinase kinase 4 (BANY.1.2.g17360)
dynactin subunit 2 (BANY.1.2.g02759)
dynactin subunit 5 (BANY.1.2.g15245)
histone acetyltransferase Tip60 isoform X6 (BANY.1.2.g17798)
insulin-like receptor (BANY.1.2.g17404)
insulin receptor-like (BANY.1.2.g17408)
mesencephalic astrocyte-derived neurotrophic factor homolog (BANY.1.2.g13689)
microtubule-associated protein futsch-like (BANY.1.2.g08693)
Microtubule-associated protein futsch (BANY.1.2.g13356)
MOB kinase activator-like 4 (BANY.1.2.g20214)
NGFI-A-binding protein homolog (BANY.1.2.g02481)
NGFI-A-binding protein homolog (BANY.1.2.g02482)
nipped-B protein (BANY.1.2.g01712)
nucleolus and neural progenitor protein-like (BANY.1.2.g05558)
prolow-density lipoprotein receptor-related protein 1-like (BANY.1.2.g14230)
protein apterous-like isoform X2 (BANY.1.2.g08342)
protein daughterless (BANY.1.2.g19105)
protein ecdysoneless homolog (BANY.1.2.g06994)
protein held out wings isoform X1 (BANY.1.2.g04186)
Protein neuralized (BANY.1.2.g20573)
protein nubbin-like (BANY.1.2.g19891)
protein smoothened (BANY.1.2.g01253)
protein split ends-like isoform X3 (BANY.1.2.g10857)
rho GTPase-activating protein 100F (BANY.1.2.g12733)
rho guanine nucleotide exchange factor 10 isoform X4 (BANY.1.2.g06255)
serine/threonine-protein kinase mig-15 isoform X1 (BANY.1.2.g26064)
trafficking protein particle complex subunit 6B (BANY.1.2.g10366)
transcription factor Adf-1-like (BANY.1.2.g03430)
transcription factor Adf-1-like (BANY.1.2.g24076)
xenotropic and polytropic retrovirus receptor 1 (BANY.1.2.g07681)
Neural Signaling
5-hydroxytryptamine receptor 1A-alpha (BANY.1.2.g12845)
acetylcholine receptor subunit alpha-like 2 (BANY.1.2.g06669)
adenylate cyclase type 8 (BANY.1.2.g03804)
ARL14 effector protein (BANY.1.2.g04285)
calcium/calmodulin-dependent protein kinase kinase 1 (BANY.1.2.g12425)
dopamine receptor 2-like (BANY.1.2.g24500)
dystrophin isoforms A/C/F/G/H like protein (BANY.1.2.g16244)
gamma-aminobutyric acid type B receptor subunit 2 isoform X3 (BANY.1.2.g21830)
glutamate receptor ionotropic, kainate 2-like (BANY.1.2.g00777)
neuroligin-4, Y-linked isoform X1 (BANY.1.2.g06479)
piezo-type mechanosensitive ion channel component isoform X1 (BANY.1.2.g11981)
potassium channel subfamily T member 2 isoform X10 (BANY.1.2.g09307)
protein unc-80 homolog isoform X10 (BANY.1.2.g05052)
regulating synaptic membrane exocytosis protein 1 isoform X1 (BANY.1.2.g10739)
sodium channel protein Nach-like (BANY.1.2.g06280)
sodium channel protein para (BANY.1.2.g00003)
synaptotagmin-16 isoform X2 (BANY.1.2.g03523)
syntaxin-5 (BANY.1.2.g06764)
syntaxin-binding protein 5 (BANY.1.2.g06385)
Tachykinin-like peptides receptor 99D (BANY.1.2.g04868)
V-type proton ATPase subunit a (BANY.1.2.g18298)
log2FC
0.25
0.50
0.75
1.00
1.25
Hormone Signaling
Ecdysteroid UDP-glucosyltransferase (BANY.1.2.g10598)
juvenile hormone binding protein an-0921 precursor (BANY.1.2.g04396)
juvenile hormone epoxide hydrolase-like (BANY.1.2.g00826)
lipid droplet-associated hydrolase (BANY.1.2.g06016)
Eye Development
adenylyl cyclase-associated protein 1 isoform X1 (BANY.1.2.g04305)
ataxin-2 homolog isoform X1 (BANY.1.2.g13668)
crb (BANY.1.2.g13186)
kto (BANY.1.2.g03604)
parafibromin (BANY.1.2.g16929)
rn (BANY.1.2.g02213)
sens (BANY.1.2.g14514)
smo (BANY.1.2.g01254)
trr (BANY.1.2.g04855)
tsr (BANY.1.2.g03106)
tyrosine-protein phosphatase Lar isoform X3 (BANY.1.2.g01608)
ubiquitin-conjugating enzyme E2-17 kDa isoform X2 (BANY.1.2.g16078)
Vision
Innexin shaking-B (BANY.1.2.g22899)
retinol dehydrogenase 11-like (BANY.1.2.g12953)

A

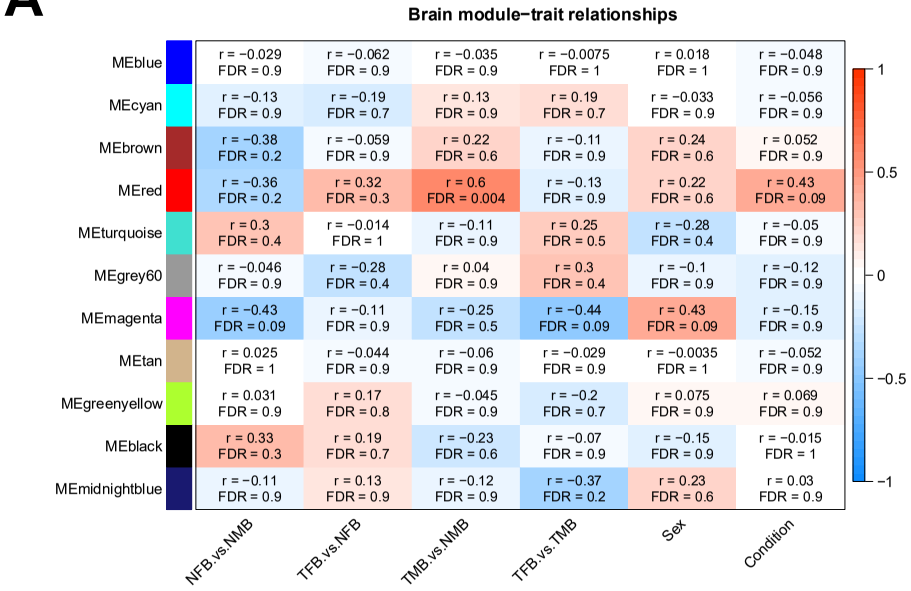

B

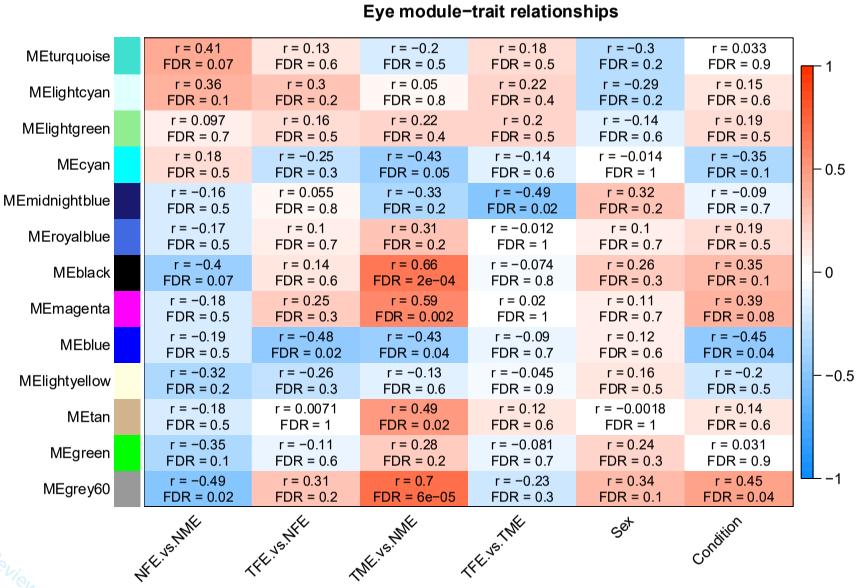

C

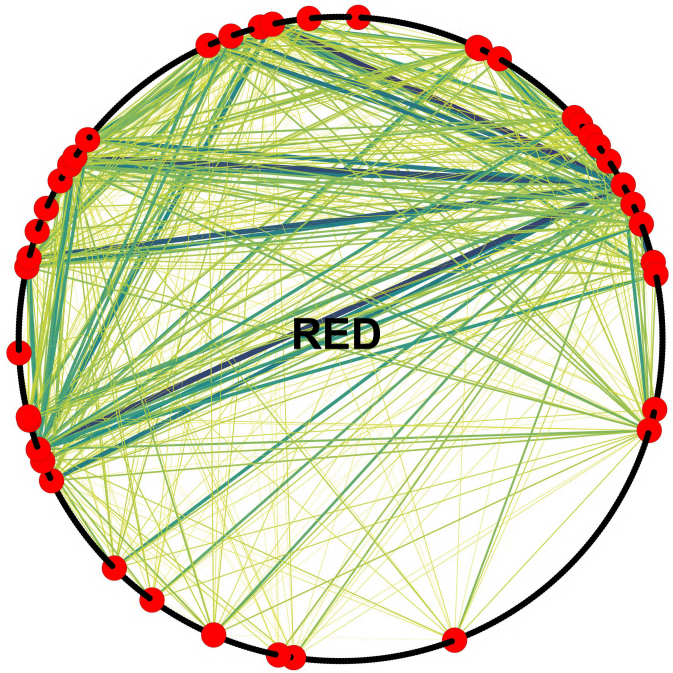

D

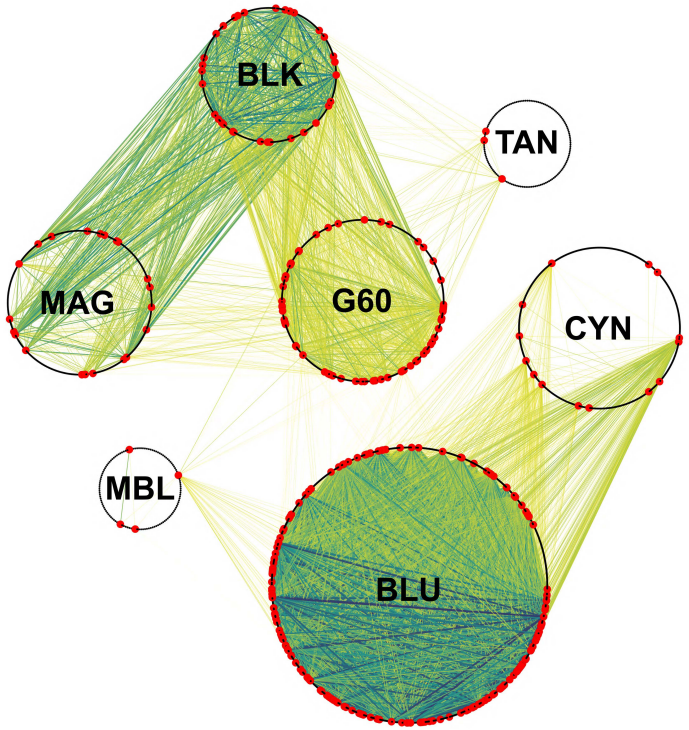

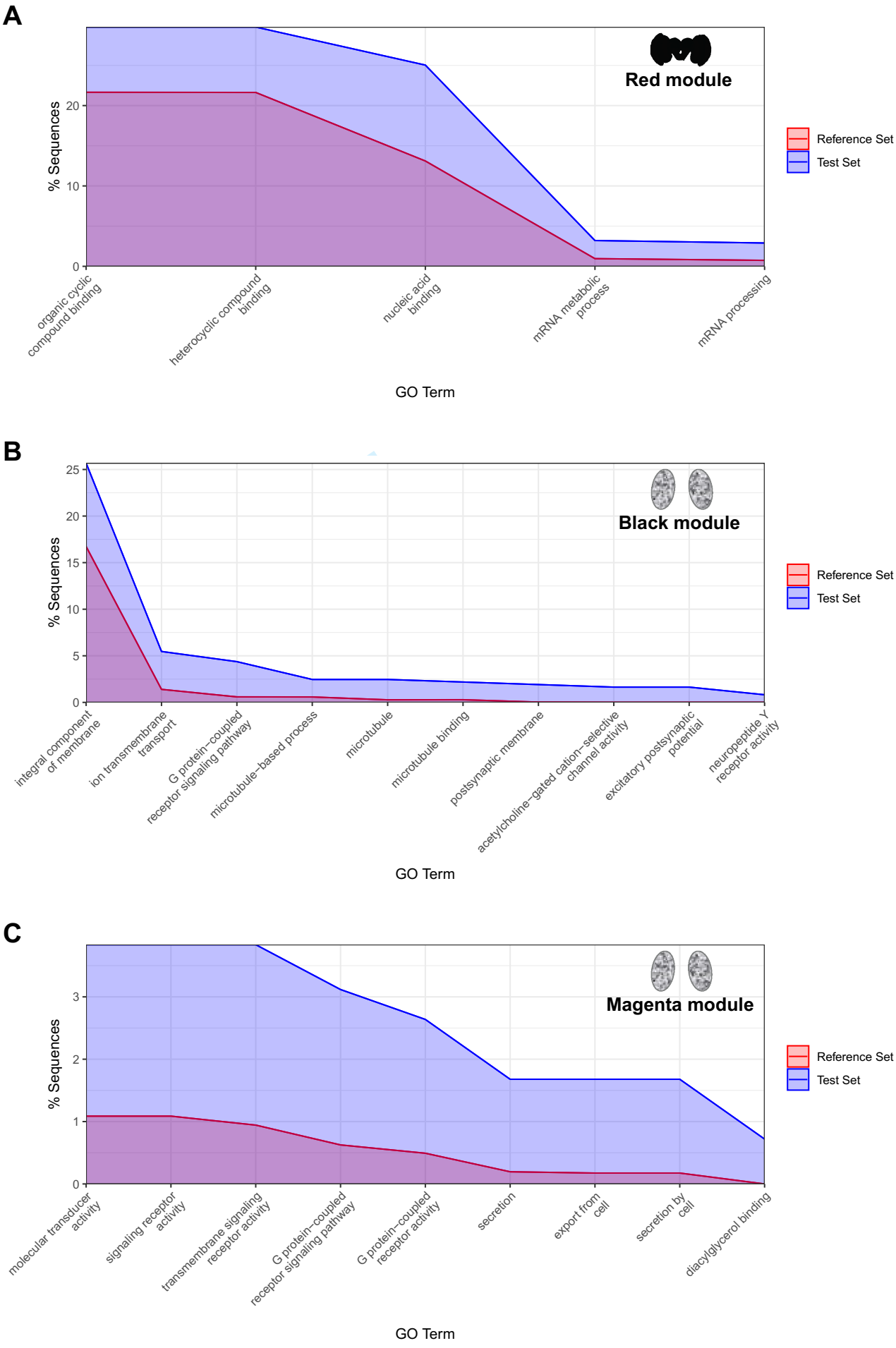
A
Red module
% Sequences
0
10
20
organic cyclic compound binding
heterocyclic compound binding
nucleic acid binding
mRNA metabolic process
mRNA processing
GO Term
Reference Set
Test Set
B
Black module
% Sequences
0
5
10
15
20
25
integral component of membrane
ion transmembrane transport
G protein−coupled receptor signaling pathway
microtubule−based process
microtubule
microtubule binding
postsynaptic membrane
acetylcholine−gated cation−selective channel activity
excitatory postsynaptic potential
neuropeptide Y receptor activity
GO Term
Reference Set
Test Set
C
Magenta module
% Sequences
0
1
2
3
molecular transducer activity
signaling receptor activity
transmembrane signaling receptor activity
G protein−coupled receptor signaling pathway
G protein−coupled receptor activity
secretion
export from cell
secretion by cell
diacylglycerol binding
GO Term
Reference Set
Test Set